

reputation of publishing good data rather than garbage. Those who insist on using students as cheap labor should at least use engineering students instead of astronomy or physics students for design and construction work.

3. OBSERVATIONAL TECHNIQUE AND DATA REDUCTION*

3.1. Atmospheric Extinction

3.1.1. Introduction

“Die enorme Bedeutung der Extinktion für die astrophysikalische Forschung ist offensichtlich. . . .”

“Die Lehre von der Extinktion ist deshalb eine der Grundlehren der Astrophysik.”

With these strong words, Schoenberg¹ introduced his discussion of extinction in the *Handbuch der Astrophysik*. Perhaps because his treatment is so impressive, little has been done since. However, the intervening forty years have brought photoelectric techniques of high precision into general use. These techniques not only allow a more accurate experimental study of extinction; they also demand a reexamination of the theoretical basis of extinction corrections, if the full accuracy of the best observations (a few thousandths of a magnitude) is to survive the process of data reduction.

Unfortunately, many observers believe that it is difficult to determine the extinction accurately, and that an accurate measurement is not necessary anyway, because mean values are adequate for photometric nights, especially in differential work. These opinions are primarily based on Stebbins and Whitford's² assertion that “it is impractical to determine the extinction thoroughly and accomplish anything else,” and Hiltner's³ statement that “the extinction is less variable than the accuracy with which it can be determined during a night when the extinction observations are interspersed with a significant number of observations on pro-

¹ E. Schoenberg, in “Handbuch der Astrophysik,” Band II, p. 1. Springer, Berlin, 1929.

² Joel Stebbins and A. E. Whitford, *Astrophys. J.* 102, 318 (1945).

³ W. A. Hiltner, *Astrophys. J. Suppl.* 2, 389 (1956).

* Part 3 is by Andrew T. Young

gram stars." Also, there is a widespread belief that stars at very large air masses must be observed in order to determine the extinction accurately.

The purpose of this part is to show how accurate extinction measurements can be made easily and without going to great air masses, and that such measurements are in fact desirable. A thorough discussion of the pitfalls of extinction measurement and correction is given, both from the observational side and from the point of view of making accurate reductions.

In order to optimize the extinction determination, it is necessary to understand the random and systematic sources of error in the observational data, and in particular their dependence on air mass. Many of these have been described in detail in previous sections, and will only be mentioned briefly here.

3.1.2. Basic Error Analyses

Initially, let us examine an idealized situation without systematic errors. We assume that the random error of a photometric measurement is a function of air mass alone, since it is common experience that the error is an increasing function of air mass.

For convenience, we shall at first assume the standard error of measurement ε is proportional to some power p of the air mass M . (More general laws will be considered later.) Thus if

$$\varepsilon = \varepsilon_0 M^p, \quad (3.1.1)$$

the statistical weight of a measurement is

$$w \propto \varepsilon^{-2} \propto M^{-2p}. \quad (3.1.2)$$

Although, in practice, this weighting is not usually taken into account, giving all data equal weight is equivalent to assuming the errors are independent of air mass, which is contrary to experience.

3.1.2.1. Two Measurements. To illustrate our general approach, suppose we try to find the extinction from just two measurements of a star, one in the zenith and the other at air mass M . If the observed magnitudes are m_1 and m_M , the extinction coefficient A is

$$A = (m_M - m_1)/(M - 1). \quad (3.1.3)$$

The error to be expected in A can be found from the law of propagation

of errors, assuming the two measurements to be independent:

$$\sigma_A^2 = [\sigma_1 \partial A / \partial m_1]^2 + [\sigma_M \partial A / \partial m_M]^2. \quad (3.1.4)$$

Equation (3.1.1) gives σ_1 and σ_M , so we find

$$\sigma_A^2 = [\varepsilon_0^2 / (M - 1)^2] (M^{2p} + 1). \quad (3.1.5)$$

Figure 1 shows the graph of Eq. (3.1.5) for a few values of p . For $p > 1$, there is a value of M for which σ_A^2 is a minimum, i.e., from which the extinction is most precisely determined. The condition for this mini-

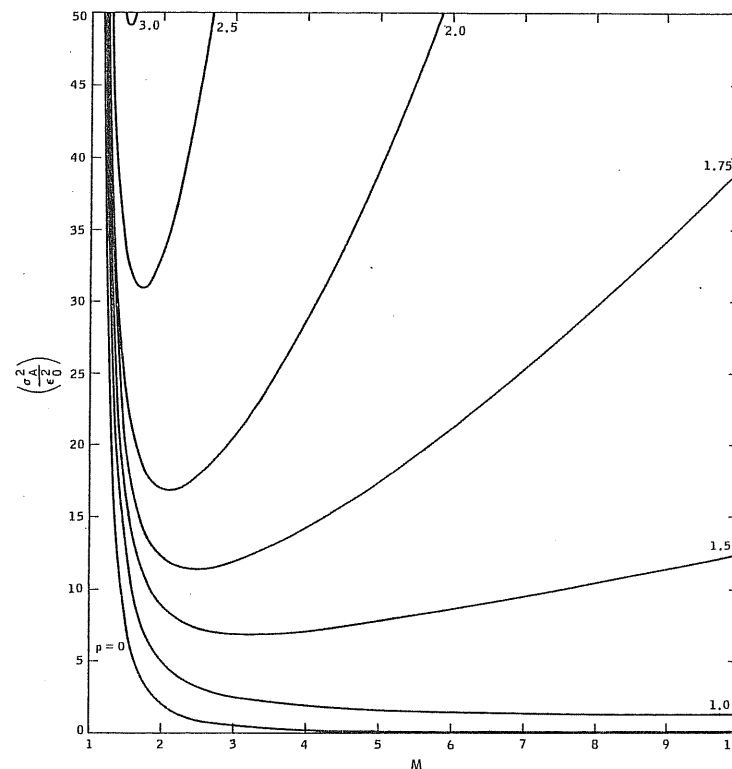


FIG. 1. Variance σ_A^2 of an extinction determination from two observations, in units of the variance of the zenith measurement ε_0^2 . The error of one observation at M air masses is assumed equal to $\varepsilon_0 M^p$ [see Eq. (3.1.5) in the text].

imum is

$$\partial(\sigma_A^2)/\partial M = 0 \quad (3.1.6)$$

or

$$0 = \varepsilon_0^2 \left[\frac{2pM^{2p-1}}{(M-1)^2} - \frac{2(M^{2p}+1)}{(M-1)^3} \right], \quad (3.1.7)$$

which reduces to

$$(p-1)M^{2p} - pM^{2p-1} - 1 = 0. \quad (3.1.8)$$

Equation (3.1.8) has no root for $p \leq 1$, so in this case M should be as large as possible. However, we shall show below that $p \approx 2$ in most cases; for $p = 2$, Eq. (3.1.8) has a root near 2.1. Thus, in this case, the extinction is best determined if the low-altitude observation is made near two air masses. At larger values, the rapid increase in σ_M more than offsets the advantage of increasing $(M-1)$; in the example, σ_A^2 is twice the minimum value if $M = 4.5$ air masses.

The above analysis indicates both the method to be used, and an important conclusion: that best results may be obtained if very large air masses are avoided.

3.1.2.2. n Measurements. From a statistical point of view, we must avoid extremely large air masses because such observations have very low weight. Thus we can improve the extinction determination if we devote more time to the observations at large M , thereby increasing the weight of the low-altitude data.

The analysis is quite similar to that used in pulse-counting to determine the optimum distribution of observing time between background and signal (see Part 1, Section 1.5.2).^{3a,b}

We thus suppose that a fraction f of the total observing time is spent at the larger air mass M_2 , and a fraction $(1-f)$ is spent at the smaller air mass M_1 (which need not, in general, be unity). If there are a total of n observations of equal duration, and ε_0 is again the standard error of a single observation in the zenith, then the mean magnitude observed near the zenith is m_1 with standard error σ_1 , where

$$\sigma_1 = \varepsilon_0 M_1^p / [(1-f)n]^{1/2} \quad (3.1.9)$$

and similarly

$$\sigma_2 = \varepsilon_0 M_2^p / (fn)^{1/2}. \quad (3.1.10)$$

^{3a} A. T. Young, *Appl. Opt.* 8, 2431 (1969).

^{3b} C. W. McCutchen, *Phil. Mag. (8th Ser.)* 2, 113 (1957).

Since

$$A = (m_2 - m_1)/(M_2 - M_1), \quad (3.1.11)$$

we have

$$\sigma_A^2 = \frac{1}{n} \left(\frac{\varepsilon_0}{M_2 - M_1} \right)^2 \left[\frac{M_1^{2p}}{(1-f)} + \frac{M_2^{2p}}{f} \right]. \quad (3.1.12)$$

Now, in order to minimize σ_A , we have, in addition to the analog of Eq. (3.1.6), the condition

$$\partial(\sigma_A^2)/\partial f = 0. \quad (3.1.13)$$

The former yields

$$(p-1)(1-f)M_2^{2p} - p(1-f)M_1M_2^{2p-1} - fM_1^{2p} = 0 \quad (3.1.14)$$

and the latter gives

$$f^2M_1^{2p} - (1-f)^2M_2^{2p} = 0. \quad (3.1.15)$$

In general, σ_A will be smallest when M_1 is as small as possible, i.e., $M_1 = 1$. This ideal can only be approached in practice; however, it can be approached rather closely, as $M_1 < 1.1$ within 24° of the zenith. We therefore adopt $M_1 = 1$ for the next part of the discussion. Even with this simplification, the conditions for minimum σ_A are rather complex

$$(p-1)(1-f)M_2^{2p} - p(1-f)M_2^{2p-1} - f = 0 \quad (3.1.16)$$

and

$$f^2 - (1-f)^2M_2^{2p} = 0. \quad (3.1.17)$$

If we solve Eq. (3.1.17) for M_2 , we find

$$M_2 = [f/(1-f)]^{1/p}. \quad (3.1.18)$$

We can then replace M_2 in Eq. (3.1.16) with Eq. (3.1.18), collect all terms involving p on one side, and raise the result to the p th power to find

$$[(pf-1)/pf]^p = (1-f)/f = M_2^{-p} \quad (3.1.19)$$

or

$$(pf-1)^p - p^p f^{p-1}(1-f) = 0. \quad (3.1.20)$$

We can solve Eqs. (3.1.18)–(3.1.20) exactly only for simple rational values of p . For example, for $p = \frac{3}{2}$ we readily find $f = \frac{3}{8}$, $M_2 = 4$; for $p = 2$, we obtain $f = (2 + 2^{1/2})/4 = 0.854$, $M_2 = 1 + 2^{1/2} = 2.414$.

In general, f can be found by solving Eq. (3.1.20) for $(1 - f)$ and iterating

$$f_{k+1} = 1 - f_k[(pf_k - 1)/pf_k]^p. \quad (3.1.21)$$

Then M_2 follows from Eq. (3.1.18). The resulting values of M and f are shown as functions of p in Fig. 2, along with the corresponding values of $(\sigma_A n^{1/2})/\epsilon_0$.

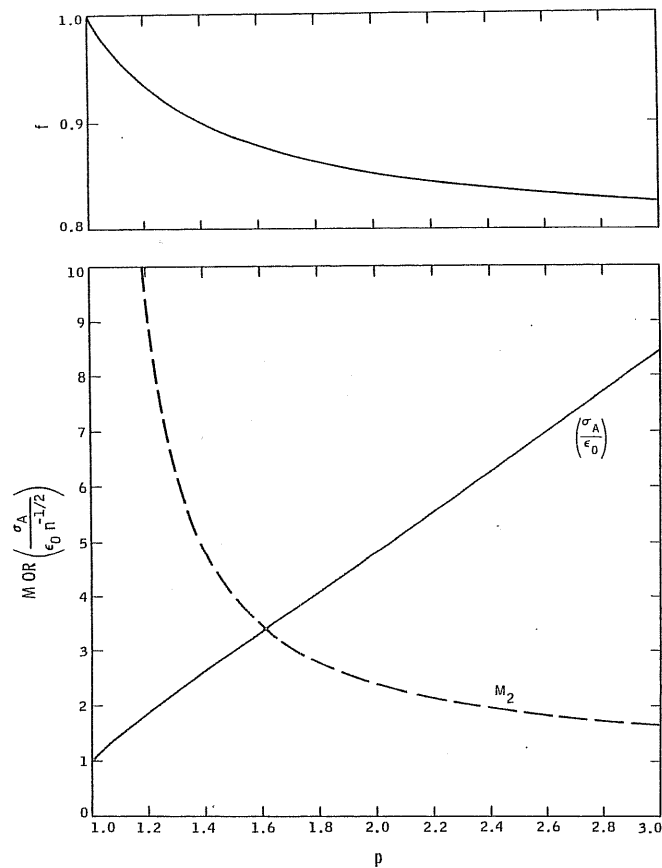


FIG. 2. Values of M_2 and f for optimum extinction determination, as functions of p . The standard deviation σ_A of the extinction coefficient is also shown for these optimum conditions, in units of $(\epsilon_0/n^{1/2})$.

In order to show how rapidly the quality of the extinction measurement deteriorates as f and M_2 deviate from their optimum values, we have computed contours of constant σ_A^2 (in units of ϵ_0^2/n) in the (f, M_2) plane. To show the results in terms of observational variables, we have plotted the contours in the (f, z) plane, assuming $M = \sec z$. These plots (see Figs. 3 and 4) show that the observations should be planned carefully in order to determine A precisely. In general, values of f near 0.8–0.9 and values of M near 2–4 (or values of z from 60 to 75°) give the best results. In particular, stars within about 10° of the horizon should be avoided.

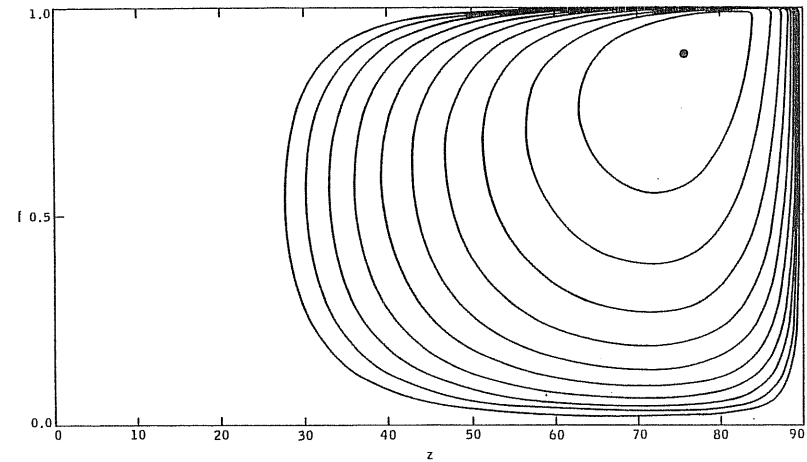


FIG. 3. Contours of equal extinction-coefficient variance σ_A^2 in units of the minimum variance, for $p = 1.5$. The contours are separated by a factor of $2^{1/2}$. Thus the weight of an extinction determination of the innermost contour is 0.707 of the weight of an extinction determination under optimum conditions (indicated by the large dot); the weight on the second contour is half the optimum; and, in general, the weight of an extinction determination along the j th contour out from the center is $1/2^{(j/2)}$ of optimum. The cut through the contoured surface along the line $f = 0.5$ corresponds to the curve for $p = 1.5$ in Fig. 1.

The following properties of Figs. 3 and 4 are of practical interest: (1) The contours are more closely spaced on the large z side of the optimum than the small z side. Thus it is safer to err in the direction of lower air masses; a 10° error in altitude is less harmful in this direction. (2) At smaller than optimum air masses, the best value of f approaches 0.5.

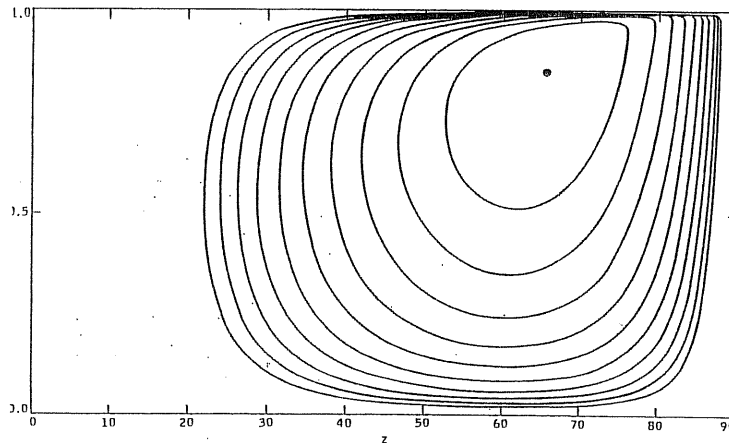


FIG. 4. Contours as in Fig. 3, but for $p = 2.0$.

Thus, (3) the common practice of observing each extinction star once on the meridian, and once each at 60 to 70° zenith distance in the east and in the west (giving $f = \frac{2}{3}$) gives a result not far from optimum. (4) The innermost contour comes very near to the line $f = 1$ in the neighborhood of $z = 60-70^\circ$. Thus it is practically impossible to have too many observations in the 2-3 air-mass range, if a few extinction stars are observed near the zenith.

Of course, the above analysis is rather idealized. In order to investigate the actual dependence of ϵ on M , and hence to determine realistic values of f and z to be used in planning observing programs, we consider the actual behavior and magnitude of both random and systematic errors in the next sections. We can then reexamine the optimization problem in more realistic terms.

3.1.3. Random Errors in Photometry

We shall consider sources of random error in order of increasing dependence on zenith distance, beginning with errors independent of air mass.

3.1.3.1. Fixed Errors. The fixed random errors are primarily instrumental, and can in principle be eliminated; but in actual practice, they are usually significant. The most obvious instrumental errors are random

variations in power supplies and amplifiers (either intrinsic, or due to line-voltage or line-frequency variations); these can be reduced to negligible levels by using well-regulated and stable units and (if line stability is a problem) line regulators—preferably of the electronic servo-regulator type rather than the simple transformer type, which are very sensitive to frequency and waveform changes.

Random changes in photomultiplier dynode gain may be caused by cesium migration within the tube. These changes are usually rather slow, and may be measured by observing a standard source. However, such sources are often so faint that photon noise from the source becomes an important cause of random error. Random dynode voltage variations may also be caused by noisy components, such as Zener diodes or carbon resistors.

Components that work well at room temperature may become noisy at low temperatures. Leakage is often a problem if water vapor is allowed to condense on sockets at low temperatures. Silica gel is a much poorer drying agent than is generally supposed; if it is used, it should be kept cold, as warm silica gel may easily have a higher water vapor pressure than a cold socket, and thus act as a source of water rather than a sink. Silica gel has also been found to emit light spontaneously, so it should be optically isolated from the photomultiplier.

Random photomultiplier temperature variations affect dynode gain and cathode spectral response. These variations are usually large and significant in dry-ice-cooled boxes,³⁰ but can be much reduced by either (a) using a heat-transfer liquid such as ethyl acetate or Freon-11 on the dry ice; (b) using water ice instead of dry ice; (c) using a servo-controlled refrigeration system; or (d) using no cooling at all. Method (a) should be used only with very noisy photomultipliers which require extreme cooling, such as 1P21s and tubes with S-1 cathodes. Method (b) is satisfactory with quiet end-on tubes such as the EMI 6256, in which the noise reaches its minimum value near 0°C;³¹ this method has been used at the Cape Observatory with good results. It is preferable to (a) because water has much higher heat capacity and latent heat of fusion than dry ice; also, there is no need to vent escaping gas, so the box can be completely closed and spillage is eliminated. Unfortunately, many cold boxes are not watertight. If these are replaced by servo-regulated systems (c), the dead-band of the system is the source of random temperature variations. If

³⁰ A. T. Young, *Appl. Opt.* 2, 51 (1963).

³¹ A. T. Young, *Rev. Sci. Instrum.* 36, 394 (1967).

cooling is abandoned altogether, the ambient temperature should be monitored, so that corrections for temperature effects can be applied. This method (d) has been used very successfully by Stock at Cerro Tololo, and is best used where the ambient temperature is nearly constant through the night.

Generally, dark noise is negligible for the bright stars used to measure extinction. However, in some photometers a spurious "dark" noise may be caused by light leaks, especially from indicator or reticle-illumination lamps within the photometer head.

A final instrumental effect is the constant reading error. This is on the order of 0.001 of full scale on strip charts,³⁰ but may become a larger fraction of a magnitude if small deflections are used. In digital systems, this error is $1/(12)^{1/2}$ of the least count (root mean square), and can be kept negligible by the use of four or more significant digits.

All the above errors can be measured by repeated observations of a constant light source during several hours. If a standard source is not part of the photometer, a well-regulated incandescent lamp can be used.

One constant source of error that is often overlooked is the uncertainty in standard-star values, if these are used to determine the extinction.⁴ For example, the internal errors of the 108 standards which define the *UBV* system⁵ are about 0.04 mag (standard error) per observation in *V*; even for stars with 5 or more observations, the estimated standard error is 0.018 mag. Considering that transformations between instrumental and standard systems are never perfect, owing to differences in passbands (and possibly to changes in the stars themselves since the standards were set up), we may adopt a constant rms error of 0.02 mag/star if Hardie's method is used. We shall return to this later.

3.1.3.2. Errors Nearly Proportional to Air Mass. The most obvious error source proportional to M is a random change in the extinction coefficient itself. That is, if A changes by ΔA , the magnitude of a star at M air masses changes by $M \Delta A$. However, it is not clear that there is any reason to expect random changes in A itself. Rather, one should expect the variable (aerosol) component of atmospheric opacity to be carried along by the atmospheric turbulence as a passive additive. In this case, the autocorrelation function of this component should decrease

³⁰ A. T. Young, *Observatory* **88**, 151 (1968).

⁴ R. H. Hardie, in "Astronomical Techniques" (W. A. Hiltner, ed.), Chapter 8, p. 178. Univ. of Chicago Press, Chicago, Illinois, 1962.

⁵ H. L. Johnson and D. L. Harris, *Astrophys. J.* **120**, 196 (1954).

with the $\frac{2}{3}$ power of the distance;^{5a} because of this correlation, deviations from the mean extinction should grow about like $M^{5/6}$. A full analysis of this problem depends on a knowledge of the outer scale of the turbulence and its variation with height, and will not be attempted here.

Near the zenith, sky brightness varies almost proportionally to M . This may be appreciable on moonlit nights, especially if large focal-plane apertures are used, or in daytime work. However, if the sky is good and sky measures are made for each star, only the photon noise from the sky should contribute a random error; this varies about as $M^{1/2}$ near the zenith. At large zenith distances, the atmosphere becomes optically thick and sky noise is nearly constant.

3.1.3.3. Errors Proportional to Higher Powers of M . As shown in Section 2.1.1.2, the low-frequency component of scintillation noise varies as the $\frac{2}{3}$ power of M near the meridian (at right angles to the upper-air winds), and as the square of M near the prime vertical (looking parallel to the wind direction). In general, the scintillation noise ε_s is given by

$$\begin{aligned}\varepsilon_s^2 &= S^2 \sec^4 z [1 + \tan^2 z \sin^2(\theta - \theta_0)]^{-1/2} \\ &= S^2 M^4 [1 + (M^2 - 1) \sin^2(\theta - \theta_0)]^{-1/2},\end{aligned}\quad (3.1.22)$$

where θ and θ_0 are the star and wind azimuths, and we again use $M \approx \sec z$. (The dependence of S on telescope aperture and other parameters was discussed previously.)

For large M , Eq. (3.1.22) is proportional to M^3 , except in a small range of θ near θ_0 . Thus, on the average, ε_s is proportional to $M^{3/2}$. If we average Eq. (3.1.22) over θ , we find

$$\begin{aligned}\overline{\varepsilon_s^2} &= (1/2\pi) \int_0^{2\pi} \varepsilon_s^2(\theta) d\theta \\ &= (2/\pi) S^2 M^4 \int_0^{\pi/2} [1 + (M^2 - 1) \sin^2 \theta]^{-1/2} d\theta \\ &= (2/\pi) S^2 M^3 K[(M^2 - 1)^{1/2}/M],\end{aligned}\quad (3.1.23)$$

where $K(x)$ is the complete elliptic integral of the first kind. Figure 5 shows the behavior of $\overline{\varepsilon_s^2}/S^2$ as a function of M , together with M^3 and M^4 for comparison. For moderate air masses, the scintillation standard

^{5a} V. I. Tatarski, "Wave Propagation in a Turbulent Medium." McGraw-Hill, New York, 1961 (reprinted in 1967 by Dover, New York).

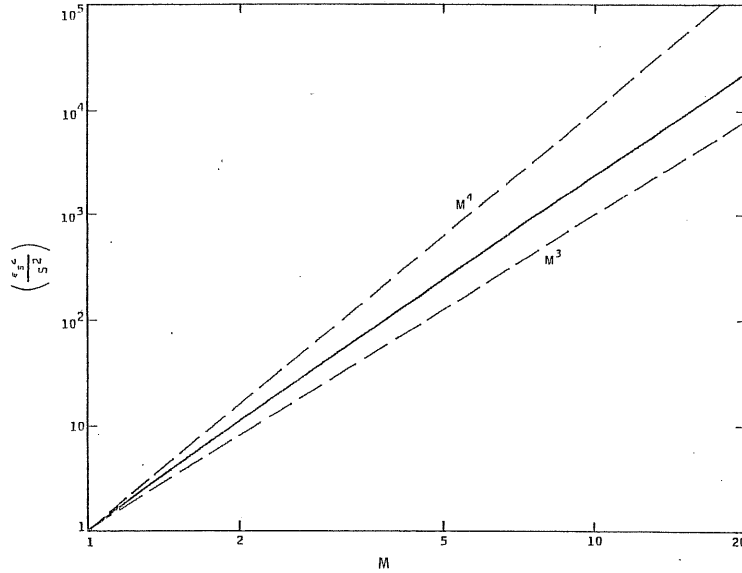


FIG. 5. Azimuth-averaged low-frequency scintillation noise as a function of air mass (log-log plot). Cubic and fourth-power laws are shown for comparison.

error is proportional to the 1.75 power of the air mass, but becomes asymptotically proportional to the $\frac{3}{2}$ power for very large air masses.

3.1.3.4. Errors Exponential in M . Since the extinction makes a star grow fainter exponentially with M , the noise due to photon statistics grows exponentially with M . For, the observed brightness of a star of apparent magnitude m is

$$I = I_0 \cdot 10^{-0.4m}, \quad (3.1.24a)$$

so we have

$$\sigma_I = CI^{1/2} = C' \cdot 10^{-0.2m}, \quad (3.1.24b)$$

for the photon noise in intensity units. The photon-noise error, in magnitudes, is

$$\begin{aligned} \varepsilon_m &= -2.5 \log_{10}[(I + \sigma_I)/I] \\ &= 1.08574 \ln(1 + \sigma_I/I) \\ &\approx 1.08574 \sigma_I/I, \end{aligned} \quad (3.1.25)$$

if $\sigma_I \ll I$. Thus

$$\varepsilon_m \approx (\text{const})10^{+0.2m} = (\text{const}) \exp(0.46052m). \quad (3.1.26)$$

However, the apparent magnitude m is a function of air mass M

$$m = m_0 + A \cdot M, \quad (3.1.27)$$

where A is the extinction coefficient and m_0 is the extra-atmospheric magnitude. Thus,

$$\varepsilon_m = (\text{const})10^{+0.2A \cdot M} = (\text{const}) \exp(0.46AM), \quad (3.1.28)$$

where we absorb the m_0 term in the exponent into the constant.

In *UBV* photometry, photon noise is generally smaller than scintillation noise for naked-eye and most HD stars at moderate air masses (cf., Table I of Part 2). However, for very large air masses, or for narrow-band systems—especially those using the low-efficiency S-1 cathode—photon noise may be important. This is generally true in spectrophotometry, where passbands as narrow as 20–50 Å are often used.

Because of the importance of this special case, we have carried through the error analysis for pure photon noise (see Fig. 6). If we have

$$\varepsilon(m_0, M) = \varepsilon_0 \exp[0.46(m_0 + AM)] = C \exp(0.46AM) \quad (3.1.29)$$

in place of Eq. (3.1.1), then

$$\sigma_A^2 = \left(\frac{C}{M_2 - M_1} \right)^2 \left[\frac{\exp(0.46AM_1)}{f^{1/2}} + \frac{\exp(0.46AM_2)}{(1-f)^{1/2}} \right]. \quad (3.1.30)$$

The minimization with respect to M_2 gives

$$[0.46A(M_2 - M_1) - 2] \exp[0.46A(M_2 - M_1)] = 2 \left(\frac{f}{1-f} \right)^{1/2}, \quad (3.1.31)$$

and that with respect to f gives

$$\exp[0.46A(M_2 - M_1)] = [f/(1-f)]^{3/2}. \quad (3.1.32)$$

The exponential factor can be eliminated by taking the ratio of Eq. (3.1.31) and (3.1.32), which leads to

$$0.46A(M_2 - M_1) = 2/f, \quad (3.1.33)$$

or

$$M_2 = M_1 + (2/0.46Af). \quad (3.1.34)$$

Combining Eqs. (3.1.32) and (3.1.33) we have

$$[f/(1-f)]^{3/2} = \exp(2/f), \quad (3.1.35)$$

whose solution is $f = 0.8322967191\dots$, independent of A . (Note that this value is similar to those found for moderate power laws.) The optimum value of M_2 then follows from Eq. (3.1.34). In general, this value is rather large; for $A \leq 1.0$, $M_2 > 6$ for $M_1 = 1$.

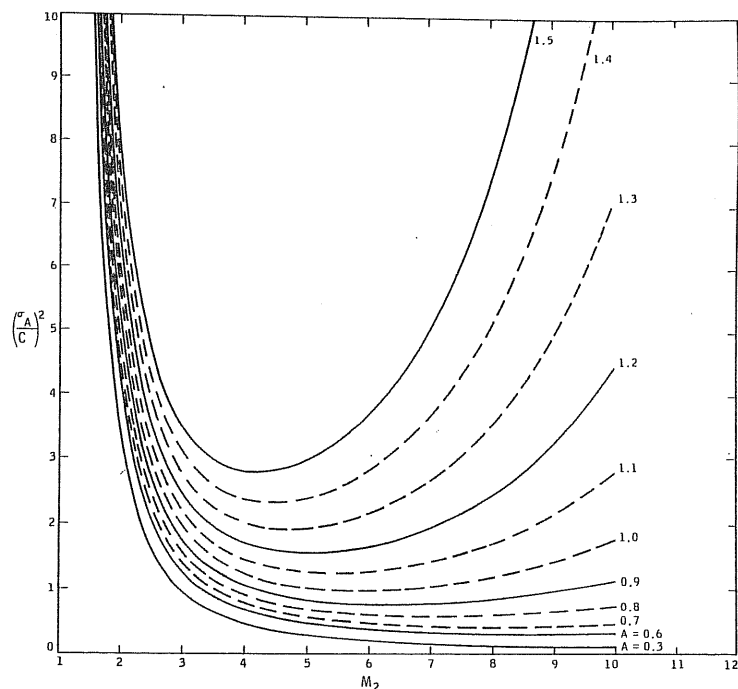


FIG. 6. Curves analogous to Fig. 1 for $f = \frac{1}{2}$ and noise due only to photon statistics. The parameter is the extinction coefficient A in magnitudes per air mass.

In practice, A is usually so small that scintillation noise dominates at moderate air masses. Of course, if photon noise is important, only the very brightest stars in the sky should be used to determine the extinction, in order to keep the observational errors low.

3.1.4. Systematic Errors in Photometry

We may generally distinguish between position-dependent and time-dependent systematic effects, although this distinction is not always clear-cut. For example, temperature effects usually show up as time-dependent errors, as the ambient temperature decreases during the night. However, instrumental temperature effects may in some cases show a positional dependence. For example, consider the case of a very poorly constructed "cold box" made of balsa wood, with only the photocell housing made of metal. When the telescope was turned so the dry ice lay against the metal cell housing, the cell rapidly cooled some tens of degrees; when the telescope pointed in other directions, the cell became much warmer. The result was large (several tenths of a magnitude) zero-point shifts, partially correlated with position.

Of course, it is absolutely necessary to have a linear photometer; otherwise, nonlinear or even "fatigue" effects, which depend on the apparent brightness of a star, will cause systematic errors correlated with air mass—especially on the brightest stars observed, which are the ones used for measuring the extinction. One should be careful about "correcting" for instrumental nonlinearities, as these corrections are likely to show significant variations with temperature, line voltage, scintillation, and other variables.

We now consider purely position-dependent and time-dependent systematic errors, in turn. (Systematic errors inherent in observational or reduction techniques will be deferred to the following section, as they are generally related to each other.)

3.1.4.1. Position-Dependent Errors. Positional systematic effects are of two types: instrumental and atmospheric. The latter are usually a function of air mass, and are therefore more difficult to detect from ordinary photometric observations.

3.1.4.1.1. MAGNETIC EFFECTS. The best-known instrumental effect is that of external magnetic fields on the photomultiplier. From data published by the manufacturers, one can estimate the magnitude of the effect for different types (see Table I). No data are available for the close-spaced EMI tubes such as the 6256 or 9502; these should be somewhat less sensitive to magnetic fields than the wide-spaced 6097. Also, no data are available on the ITT tubes (FW-118, -130, etc.), but experience indicates they are similar in magnetic sensitivity to the EMI box-and-grid tubes (9524, etc.). In some cases, the effect differs by an

TABLE I. Magnetic Effects in Photomultipliers

Type	Dynode system	Response change to 1-G field (%)	Field required for 1% response change (G)
RCA 1P21	Focused, squirrel-cage	5	0.2
RCA 8575	Linear focused	40	0.15
EMI 6097	Unfocused, venetian-blind	5	0.2
EMI 9524	Unfocused, box-and-grid	10	0.4

order of magnitude from one field orientation to another; the table is based on the direction of maximum effect.

The earth's field is on the order of $\frac{1}{3}$ to $\frac{1}{2}$ G, depending on the location of the observer. However, owing to magnetization of the telescope and dome, considerably larger fields may occur at the photometer. In general, fields must be kept below 0.1 G. The adequacy of magnetic shielding can be checked by looking at a standard source while moving either telescope or dome.

3.1.4.1.2. GRAVITATIONAL EFFECTS. Gravitational effects may result from flexure in the telescope or photometer, or even within the photomultiplier. For example, Moreno⁶ has reported a position-dependent error within the photometer amounting to 0.02 mag.

Flexure effects within a photomultiplier may be due to sagging of grid wires or motion of the entire multiplier structure within the envelope; a tube that "clunks" when shaken gently from side to side should be rejected. Such flexures can be detected by moving the telescope while looking at a standard source, and cannot be distinguished from magnetic effects without further tests. However, some standard sources may also show gravitational effects: loose particles of phosphor may migrate within sealed, radioactively excited sources.

3.1.4.1.3. DIFFRACTION PLUS SEEING AND DISPERSION. Another important class of errors results from the exclusion of some of the measured star's light by the focal-plane diaphragm. These effects are discussed in Section 2.1.1.

⁶ H. Moreno, *Astron. Astrophys.* 12, 442 (1971).

3.1.4.1.4. REFRACTION EFFECTS. Dispersion is not the only source of systematic error due to atmospheric refraction. In principle, one should also consider the foreshortening of the telescope aperture at large zenith distances, somewhat like the foreshortening of a penny seen obliquely at the bottom of a glass of water. This causes the vertical extent of the extra-atmospheric bundle of rays intercepted by the telescope to be reduced by a factor equal to the cosine of the atmospheric refraction. However, even at the horizon, the refraction is only about half a degree, so this factor always lies between unity and $\cos 35 \text{ arcmin} = 0.99995$. The maximum systematic error is thus 0.00005 mag, so this effect can safely be neglected.

A more serious error of the same general kind arises because all objects have a finite angular extent. In this case, the differential refraction between upper and lower limbs reduces the solid angle subtended by the object. Since no optical system (such as the atmosphere) can increase the surface brightness of an object, the total stellar magnitude becomes fainter.[†] In the flat-earth approximation, the refraction is $r(z) = (n - 1) \tan z$, and the compression of a small disk of diameter D is

$$\begin{aligned} \Delta D &= D(n - 1) d(\tan z)/dz \\ &= D(n - 1) \sec^2 z = D \cdot M^2(n - 1), \end{aligned} \quad (3.1.36)$$

where n is the atmospheric refractive index. Since $(n - 1) \approx 3 \times 10^{-4}$, the *fractional* change, which is nearly equal to the error in magnitudes, is

$$\Delta D/D \approx (3 \times 10^{-4}) M^2. \quad (3.1.37)$$

This amounts to a hundredth of a magnitude at about 6 air masses, and rapidly increases beyond that. For visual light, where the extinction is about 0.2 mag per air mass, this effect is equivalent to an air-mass error of 0.05 at $z = 80^\circ$. Thus, the contribution of the refraction effect to the apparent extinction is quite comparable to many of the high-order correction terms ordinarily included in air-mass calculations. From an optical point of view, it may be regarded as a weak barrel-distortion of the entire sky; in effect, the atmosphere acts like a weak fish-eye lens, with its axis vertical.

[†] This effect is an example of the differential refraction that dims a star during an occultation by a planet; looking toward the earth's horizon is looking at the limb of our planet.

3.1.4.2. Time-dependent Errors

3.1.4.2.1. INSTRUMENTAL DRIFT. Systematic errors of this type are often associated with instrumental temperature drifts. Temperature effects in photomultipliers and in filters have already been discussed. As was emphasized earlier, most photomultipliers have long thermal time constants; typically, 3 or 4 hr should elapse between the beginning of cooling and the beginning of observations. The only real solution is to use a reliable standard source (preferably, thermostatically controlled—see Section 2.2).

3.1.4.2.2. VARIABLE EXTINCTION. A common time-dependent problem is the slow change of the extinction coefficient itself. This usually appears as a gradual decrease in the extinction during the night, owing to a slow fallout of the aerosol component. The reverse effect appears during the day, as convection caused by solar heating mixes aerosols produced near ground level into the lowest few kilometers of the atmosphere. This is visible as the growth in size and brightness of the solar aureole from morning until late afternoon.⁷ Sometimes the extinction change can be represented as a linear function of time, at least over a few hours. In general, the only safe policy is to observe enough extinction stars to maintain a nearly continuous check on the course of the extinction coefficient.

A convenient method has been described by Young and Irvine.^{7a} In this program, each measurement is weighted by $1/\sec z$, so that the residuals have the dimensions of an extinction coefficient (i.e., magnitudes per air mass). Thus, a simple plot of residual vs. time gives a picture of the deviations, if any, from the mean extinction. Because data from several nights are reduced together, any star observed more than once serves as an extinction star, so that a good record of any variation is obtained. Nights with variable extinction automatically receive lower weight than those with constant extinction. Finally, one can use the time-dependent residual plots to interpolate an improved extinction coefficient, and correct the results. A somewhat similar procedure is used by Nikonov and Nikonova,⁸ and by Rufener.⁹

A problem closely related to temporal changes in extinction is an azimuth dependence. One must first of all be careful to distinguish between

⁷ A. T. Young and L. G. Young, *Sky Telescope* 43, 140 (1972).

^{7a} A. T. Young and W. M. Irvine, *Astron. J.* 72, 945 (1967).

⁸ V. B. Nikonov and E. K. Nikonova, *Izv. Krim. Astrofiz. Obs.* 9, 41 (1952).

⁹ F. Rufener, *Publ. Obs. Genève, Ser. A* No. 66 (1964).

a genuine positional variation in extinction, and a positional variation in instrumental response, such as might be due to magnetic or gravitational effects. In particular, apparent gradients or asymmetries are less likely to occur in uniform terrain than near cities or bodies of water, and are likely to be due to instrumental rather than atmospheric effects if there is no obvious geographic cause near at hand. As the variable extinction is due to aerosols, which usually^{9a,b} have scale heights less than 3 km, more typically close to 1.3 km, even in the daytime, any real asymmetry must be quite local—say, within 10 km of the telescope. Unless maintained by local sources and sinks, any irregularities will simply be carried away by the wind in a short time. For example, assume a patch of aerosol at 2-km height and a 3-m/sec wind, which is typical at this height. This patch moves from the zenith to two air masses in 19 min, to three air masses in 31 min, and to four air masses in 43 min. Thus, the time required to pass across the whole useful area of sky is typically an hour or less. One must therefore regard with suspicion reports of general extinction gradients lasting several hours at remote locations; an instrumental problem seems much more likely.

Even if a time-varying extinction is due to advection of air with different aerosol content, not much asymmetry across the sky is to be expected. For example, assume the rather large extinction change of 0.02 mag/air mass per hour. With the same wind model (3 m/sec \approx 10 km/hr), the horizontal separation between points at $\sec z = 2.0$ at 2 km height on opposite sides of the sky is only 7 km, which is traversed in about 40 min. Thus, the difference in extinction coefficient between these two points would be less than 0.015 mag/air mass, even if the aerosol were all concentrated at 2-km height. As the aerosol is usually much more concentrated toward the ground, the east–west extinction gradient would generally be much less than 0.01 mag/air mass per (effective) scale height, even in this rather extreme case. Thus, it is sufficiently good to assume an extinction that is uniform over the sky, even when appreciable variations occur with time.

At first, it seems difficult to distinguish among a changing extinction coefficient, an east–west asymmetry, and an instrumental drift, as all three are strongly correlated with time. However, it appears possible, at least in principle, to diagnose the problem from the shape of the Bouguer plot. Consider first a uniform east–west gradient in the ex-

^{9a} L. Elterman, R. Wexler, and D. T. Chang, *Appl. Opt.* 8, 893 (1969).

^{9b} A. E. S. Green, A. Deepak, and B. J. Lipofsky, *Appl. Opt.* 10, 1263 (1971).

tion. Assume the extinction coefficient varies linearly with horizontal distance; then, since the horizontal displacement of the line of sight at each height is proportional to $\tan z$ (in the direction of the gradient), the apparent magnitude of a star is

$$m = m_0 + (A_0 + A_1 \tan z) \sec z \quad (3.1.38)$$

in the flat-earth approximation. Here m_0 is the outside-the-atmosphere magnitude. (This formula also assumes the star is confined to the prime vertical, i.e., it is exact only for observatories at the terrestrial equator. However, it illustrates the phenomenon fairly well, even for moderate

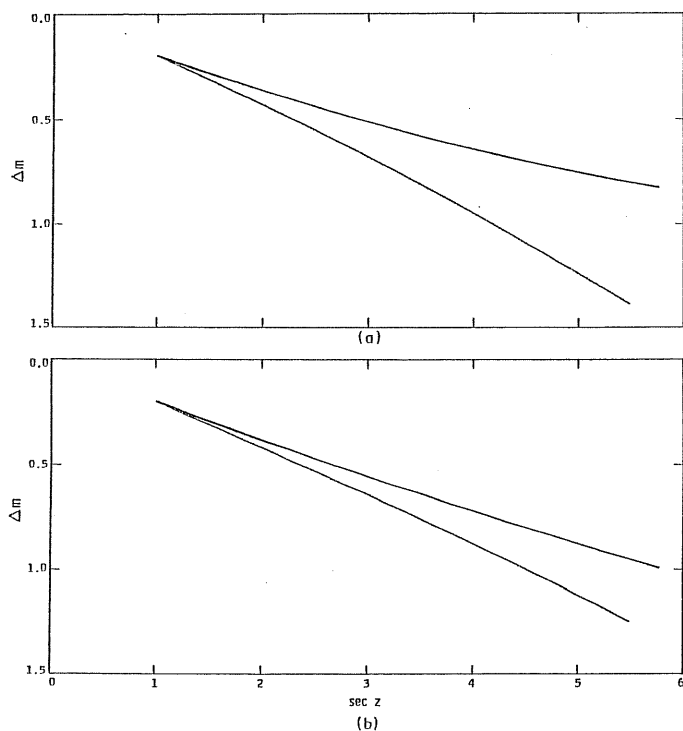


FIG. 7. Bouguer plots for a horizontal extinction gradient [see Eq. (3.1.38)]. Gradients of 0.01 and 0.005 mag/air mass/scale height are shown. (a) $A_0 = 0.2$, $A_1 = 0.01$; (b) $A_0 = 0.2$, $A_1 = 0.005$.

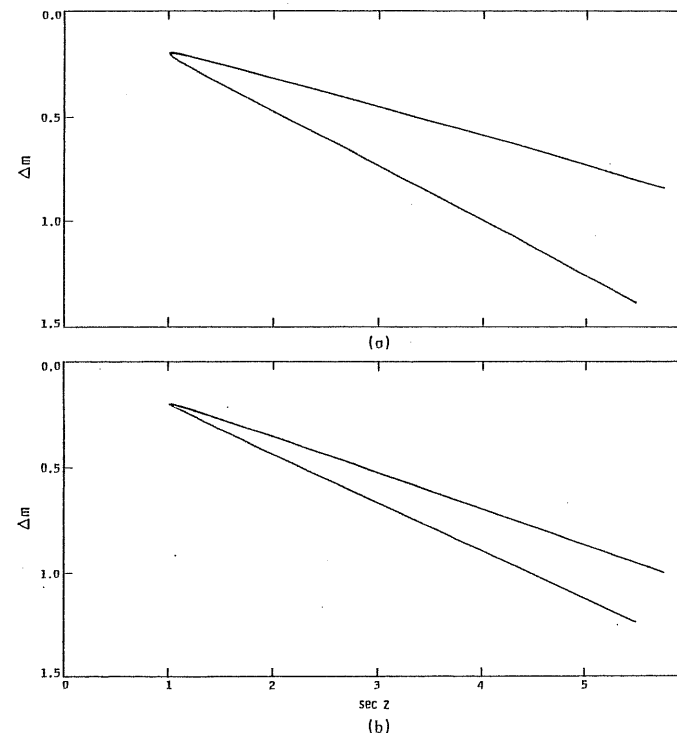


FIG. 8. Bouguer plots for a time-varying extinction coefficient [see Eq. (3.1.39)]. Variations of 0.01 and 0.005 mag/air mass/hr are shown. (a) $A_0 = 0.2$, $A_1 = 0.01$; (b) $A_0 = 0.2$, $A_1 = 0.005$.

latitudes.) The results are shown in Fig. 7. Alternatively, suppose the extinction coefficient varies linearly with time, but is the same all over the sky. Then

$$\Delta m = m - m_0 = (A_0 + A_1 t) \sec z. \quad (3.1.39)$$

With the same assumptions as before, the hour angle t is just the zenith distance z (see Fig. 8). Finally, an instrumental drift linear in time gives (Fig. 9)

$$\Delta m = A_0 \sec z + A_1 t. \quad (3.1.40)$$

The three alternatives may be distinguished by the shapes of their Bou-

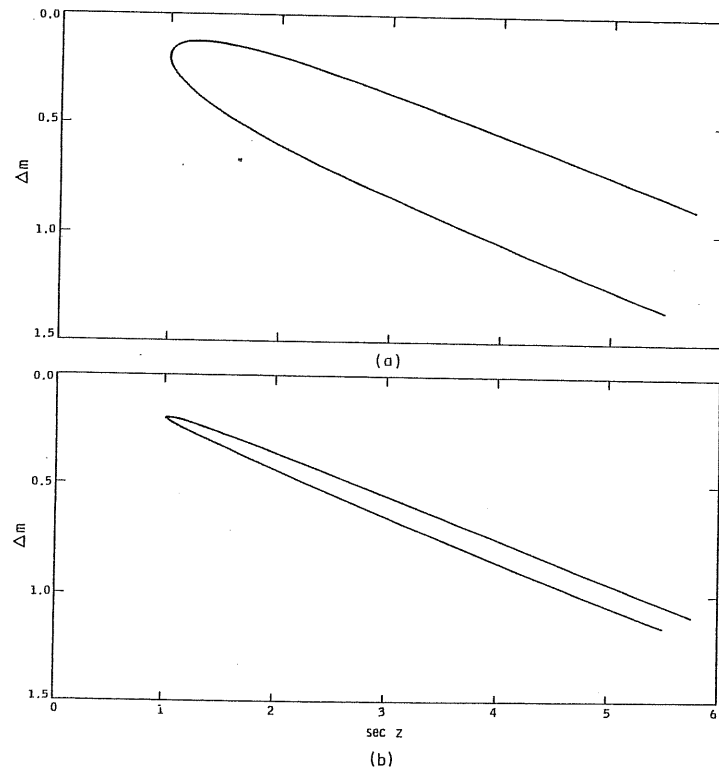


FIG. 9. Bouguer plots for instrumental drifts of 0.05 and 0.01 mag/hr [see Eq. (3.1.40)]. (a) $A_0 = 0.2$, $A_1 = 0.05$; (b) $A_0 = 0.2$, $A_1 = 0.01$.

guer curves, especially near the meridian. The east-west gradient gives two branches convex toward each other, meeting at a cusp with a common tangent. The time-dependent extinction coefficient gives two nearly straight lines, meeting at an angle. The instrumental drift gives two nearly parallel curves, concave toward each other, and joined by a rounded bend.

The time-dependent curves look more familiar to observers than the curve with asymmetry in the extinction. In particular, Fig. 8 (time-varying extinction coefficient) closely fits Code's¹⁰ description: "At Cape

¹⁰ A. D. Code, in *Proc. NSF Astronom. Photoelec. Conf.* (J. B. Irwin, ed.), p. 79, Aug. 13-Sept. 1, 1953.

Town during the winter there was almost a consistent extinction curve, or rather, curves. On the east side of the meridian one nice straight extinction curve and on the west side another nice straight but steeper extinction curve. You could almost count on this difference which was of the order of a tenth of a magnitude." (The increase of extinction at night near the city in winter is probably due to the low-grade coal that is burned for space heating in South Africa.)

Obviously, it is easier to distinguish among the three effects just discussed if several extinction stars, well distributed in hour angle, are used. For example, a drifting zero point produces the same magnitude residuals at small and large air masses, but a changing extinction coefficient affects low-altitude data more than high ones. (However, the differences may be obscured by other errors at large z .) Also, the simple linear changes shown in Figs. 7-9 are eliminated if the observations are symmetrically disposed with respect to the meridian, i.e., the least-squares value of the extinction coefficient is just A_0 in each case. In actual fact, things do not change linearly, and observations are not made symmetrically, so some systematic error will result. Furthermore, other related effects may contribute to systematic errors; for example, any north-south asymmetry in extinction would, in general, lead to a wrong value of A .

As is well known, the least-squares analysis of data leads to wrong answers (i.e., systematic errors in the results) not only if there are systematic errors in the observations, but also if the mathematical model used does not conform to the real situation. This type of error is so important that it deserves a separate section.

3.1.5. Errors in Reduction Methods

As there are many possible errors that can be introduced by inappropriate methods of analysis, we shall try to cover the most general ones first, and then treat a few specific examples of more specialized errors.

3.1.5.1. Errors in the Extinction Model. These errors may be classified as either monochromatic or wide band.

3.1.5.1.1. VIOLATION OF BOUGUER'S LAW. The refraction effects discussed in Section 3.1.4.1.4 constitute a diminution in measured brightness that is not included in Bouguer's law. We hesitate to call them "extinction," as they are not due to absorption or scattering. Because they do not represent the removal of energy from a beam of light, but rather

a change in the area and solid angle occupied by the beam, we have treated them as an observational error. They do not vary with the zenith extinction. It seems best to avoid them by keeping to small air masses.

3.1.5.1.2. ERRORS IN CALCULATING THE AIR MASS. For a long time, Bemporad's work¹¹ on the air mass, which includes curvature of the atmosphere and curvature of the ray path due to refraction, has been accepted as definitive. This is true only insofar as the extinction is proportional to the actual mass of air traversed by the ray, as is true for Rayleigh scattering. However, large contributions to the extinction are made by aerosols, water vapor, and ozone, which are by no means uniformly mixed. For example, in red light over half the extinction is due to aerosols, which typically have a scale height on the order of a kilometer.^{9a,b} Thus, Bemporad's tables (and interpolation formulas based on them, such as Hardie's⁴) must grossly overestimate the curvature corrections for red light: the scattering material is a thinner (flatter) layer than assumed, so $\sec z$ is a better approximation here. On the other hand, ozone contributes significantly between 5000 and 7000 Å, and below 13400, but is mostly concentrated near 30-km height. Thus Bemporad's work tends to underestimate the corrections to $\sec z$ in this case. Furthermore, volcanic eruptions have occasionally deposited significant amounts of aerosols in the stratosphere; these require an "air-mass" modification like ozone. Lest it be supposed that these effects are minor, we must point out that the vertical distribution of ozone¹² can be inferred, on a practical basis, from a method that depends on deviations of the ozone extinction from a $\sec z$ law.[†]

In principle it would be possible to generate modified air-mass (perhaps one should say "extinction-mass") tables for each wavelength, given the vertical distributions and extinction coefficients for all the important components. Unfortunately, the reason extinction measurements are

¹¹ A. Bemporad, *Zur Theorie der Extinktion des Lichtes in der Erdatmosphäre*, Heidelberg Mitt. No. 4 (1904).

¹² A. E. S. Green, "The Middle Ultraviolet: Its Science and Technology," p. 94. Wiley, New York, 1966.

[†] In fact, even Bemporad's investigation of the extinction was largely motivated by hopes of using it to study the constitution of the atmosphere: "Es liegt nun nahe, dass man in dieser Beziehung noch mehr von der Extinktion erwarten kann, welche im Zusammenhang mit dem atmosphärischen Zustand unvergleichlich grössere Veränderungen als die Refraktion erleidet." (Ref. 11, p. 1.)

necessary in the first place is that major components like ozone and dust are variable, so that the corrections to Bemporad's theory are also variable.

However, Abbot *et al.*^{13a} have attempted to correct Bemporad's air masses by assuming that the non-Rayleigh component of extinction is in a very thin layer near the ground, so that it can be represented by the simple $\sec z$ approximation.

In order to indicate the approximate size of such corrections, it suffices to use just the leading terms in the theory, and see how much these are affected. For instance, the air mass for an exponential spherical atmosphere of radius R and scale height h is very nearly¹³

$$M(z) = \left(\frac{\pi R}{2h}\right)^{1/2} \exp\left(\frac{R \cos^2 z}{2h}\right) \operatorname{erfc}\left[\left(\frac{R \cos^2 z}{2h}\right)^{1/2}\right], \quad (3.1.41)$$

neglecting refraction. Since the ray curvature due to refraction is only about $\frac{1}{4}$ of the curvature of the earth,¹⁴ we can allow approximately for refraction simply by increasing R by about $\frac{1}{4}$. To show the accuracy of this approximation, Fig. 10 compares $[M(z) - \sec z]$ computed from Eq. (3.1.41) (with $R = 7400$ km, and $h = 8$ km) with the corresponding values from Bemporad (which were subsequently reproduced by Schoenberg¹ and Allen^{14a}). For comparison, values calculated from Hardie's⁴ interpolation formula are also given. The exponential model can be made to fit Bemporad's results very accurately by fudging the radius of curvature slightly; $R = 8500$ km gives errors of only a few thousandths of an air mass up to $\sec z = 10$, although slightly better results are obtained at small air masses with even larger values of R . Because of the excellent fit over a wide range, the ($h = 8$, $R = 8500$) model will be used for comparisons with ozone and aerosol models having a different vertical distribution of extinction.

For the aerosol model, an aerosol with scale height of 1 km is assumed to contribute $\frac{2}{3}$ of the total extinction. The extinction-mass difference between this model and the standard model is shown in Fig. 11. In this

^{13a} C. G. Abbot, F. E. Fowle, and L. B. Aldrich, *Astr. Astrophys. Obs. Smithsonian Inst.* 4, 335 (1922).

¹³ A. T. Young, *Icarus* 11, 1 (1969). See also Ref. 12, p. 147.

¹⁴ S. Newcomb, "A Compendium of Spherical Astronomy," p. 199. Macmillan, New York, 1909.

^{14a} C. W. Allen, "Astrophysical Quantities," 2nd ed., p. 122. Univ. of London, London, 1963.

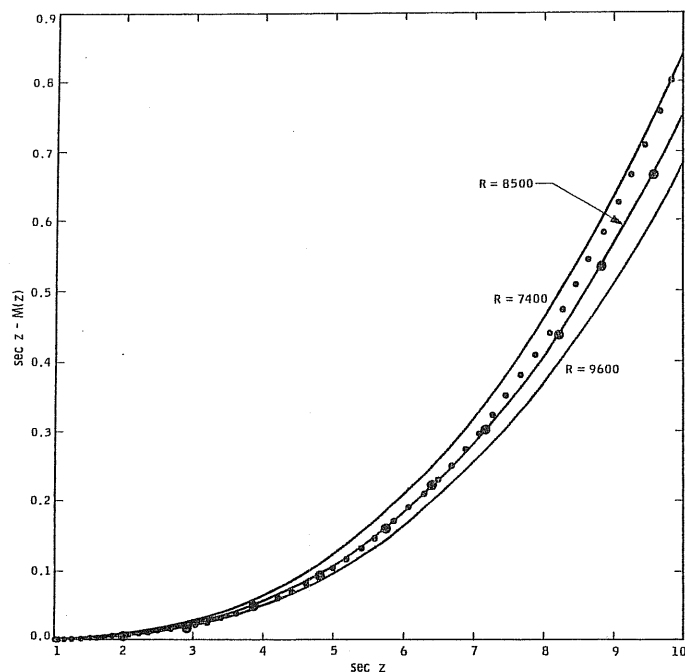


FIG. 10. Air-mass corrections to $(\sec z)$ from Bemporad's tables (large dots), from Hardie's interpolation formula (small dots), and values calculated for exponential atmospheres with 8-km scale height and radii of 7400, 8500, and 9600 km (solid curves).

case, the standard (Bemporad) model is in error by 0.01 air mass at $\sec z = 2.65$, and by 0.05 at $\sec z = 4.6$; a 1% systematic error is made in the extinction if an observation in the zenith is combined with one at $\sec z = 3.74$, owing solely to the deviation of the effective air mass from that for pure air.

For the ozone model, it suffices to assume a thin layer at height $h^* \approx 30$ km. In this case, the air path through the ozone layer is simply $\sec \zeta$, where ζ is the local zenith angle where the line of sight intersects the layer (see Fig. 1 of Ref. 13). Again absorbing refraction effects into the enlarged value for R , we have

$$\sec \zeta = (R + h^*)[(R + h^*)^2 - (R \sin z)^2]^{-1/2}. \quad (3.142)$$

In this case, let us assume the ozone contributes one quarter of the total extinction, as it does near $\lambda 3200$, and again in the Chappuis bands near $\lambda 5800$. The deviations of this model from the standard model are also shown in Fig. 11. The Bemporad values are in error by about the same amount as before, but in the opposite sense.

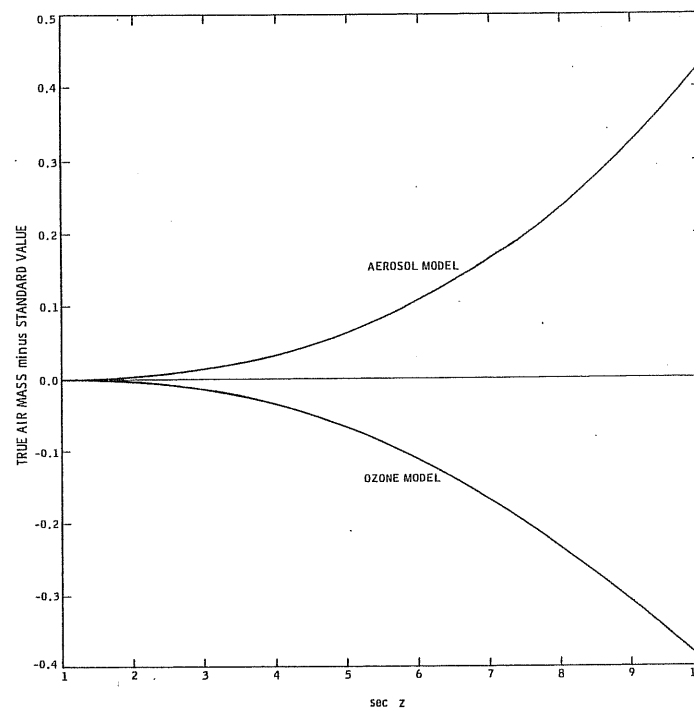


FIG. 11. Differences in effective air mass between the aerosol and ozone models described in the text, and the exponential model ($R = 8500$, $h = 8$) that closely matches Bemporad's theory.

Because the Bemporad values are in error in opposite directions, depending on whether ozone or low-level aerosols are more important, they are a good compromise. However, comparison of Fig. 10 with Fig. 11 shows that the air masses for different wavelengths can differ from each other by as much as the Bemporad air masses themselves differ from $\sec z$. The implied high precision of the tables, and of high-order

interpolation formulae such as Hardie's is therefore largely illusory.[†] The problem is not alleviated by going from sea level to high-altitude observatories, because the ozone (being almost entirely contained above the stratosphere) becomes relatively *more* important as the Rayleigh and dust contributions diminish.

It does not seem practical to devise wavelength-dependent air-mass tables, as these would depend on both the (unknown) amounts and vertical distributions of the variable components. The only way to avoid systematic errors is to stay in the region where the terms depending on the vertical distributions remain unimportant. This means keeping to air masses less than about 2.3 if the wavelength variations in $(M - 1)$ are to be kept below 1% (see Fig. 11). By $\sec z = 4$, the wavelength-dependent differences in $(M - 1)$ exceed 5%, which corresponds to a systematic error of at least 0.01 mag in reducing V to outside the atmosphere, and even larger errors at shorter wavelengths. This may partly account for the large systematic differences between different observers' absolute-energy calibrations of stars in the Balmer continuum, which practically coincides with the region where ozone absorption is important.

A further cause of systematic error is misuse of Bemporad's air-mass tables. It must be remembered that the argument in these tables is *apparent*, not true, zenith distance. Thus, if the true zenith distance is calculated from the time and the coordinates of star and observer, the refraction should be added before entering the tables. Figure 12a shows the air-mass error committed by using the true zenith distance, instead of the refracted zenith distance, as the argument in Bemporad's tables. The error reaches 0.01 at about three and a half air masses.[‡]

However, in computer work it is often convenient to use the true zenith distance. In this case the correction ($\sec z - \text{air mass}$) has the form

[†] It is clear that, in spite of subsequent opinions to the contrary, Bemporad regarded his work as anything but definitive. In the introduction to his paper, he says: "Ich brauche kaum zu betonen, dass die hier vorgeschlagene Theorie nur als eine erste Annäherung der Auflösung eines sehr verwickelten Problems anzusehen ist." He was also aware of the aerosol problem. After mentioning the then-current idea that poor transparency of the lower atmosphere was an abnormal condition, he says: "Obwohl wir nicht ganz dieser Meinung sind und lieber eine geringere Durchlässigkeit der unteren Schichten fast als normal ansehen möchten, so werden wir doch in der allgemeinen Entwicklung der Theorie die Hypothese der Konstanz des spezifischen Absorptionsvermögens beibehalten, aber nur in dem Sinne, dass dies eine erste Annäherung für die Auflösung des Problems bildet." (Ref. 11, pp. 1 and 4, respectively.)

[‡] Bemporad's corrections for temperature and pressure are often overlooked also, though they can readily exceed 1% of the air mass.

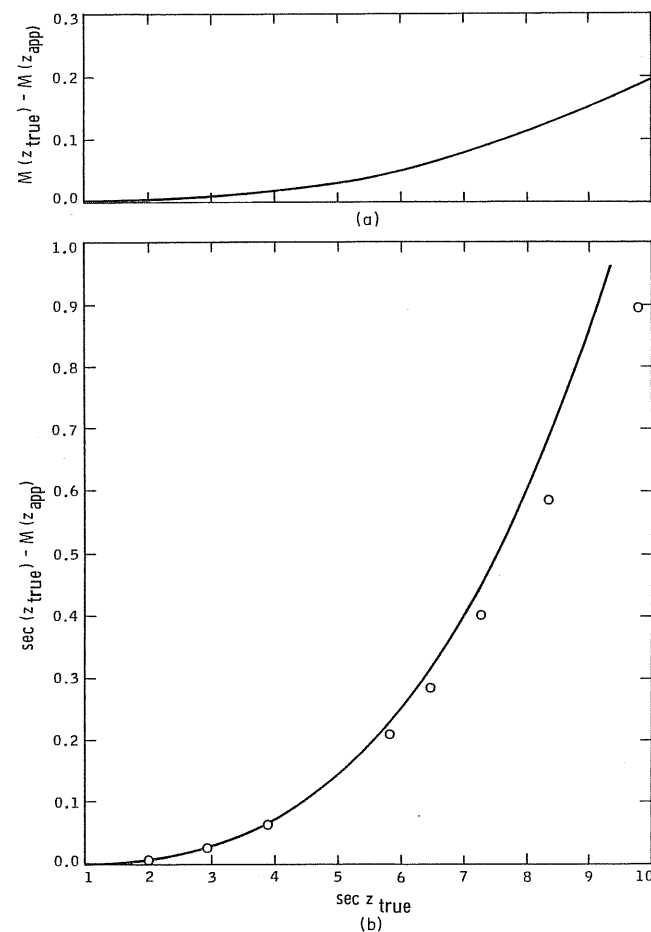


FIG. 12. (a) Error caused by using true instead of apparent zenith distance as argument in Bemporad's tables, as a function of $\sec z_{\text{true}}$; (b) Points: difference between ($\sec z_{\text{true}}$) and actual air mass from Bemporad's tables, as a function of $\sec z_{\text{true}}$. (The apparent zenith distance, including refraction, is used as argument to the tables.) The continuous curve is Eq. (3.1.43) in the text. Note that both the abscissa and the ordinate differ from those of Fig. 10.

shown in Fig. 12b, where Bemporad's values are plotted against the secant of the *true* zenith distance. Up to $\sec z_{\text{true}} = 4$, these values are well represented by the very simple formula

$$M(z_{\text{true}}) = \sec z [1 - 0.0012(\sec^2 z - 1)], \quad (3.1.43)$$

which has been used by Young and Irvine^{7a} for this purpose. [The same form has also been used by Rufener⁹ for $M(z_{\text{app}})$.] From the foregoing discussion, it should be clear that air masses greater than 4 should be avoided because of large random and systematic errors; therefore this formula is good enough for all practical work.[†]

3.1.5.1.3. PROBLEMS CONNECTED WITH COLORS. Two classes of errors are included here: (a) those associated with the measurement and reduction of colors instead of magnitudes, and (b) those due to bandwidth effects, which appear as color-dependent terms in the extinction.

It is often claimed that there are advantages to forming colors from the raw observations, and treating these as the observed quantities in the extinction corrections, instead of reducing magnitudes to outside the atmosphere and then forming colors from their differences. Some of the supposed advantages are fictitious; but some real advantages have escaped notice.

In the first place, it is essential that the observed quantities really be colors. This requires all the different wavelengths to be measured through the same air mass. This is most easily done if simultaneous observations are made with a multichannel instrument, which has the further advantage that most of the scintillation noise, which is strongly correlated between bands when small zenith angles and large apertures are used, cancels out. It should thus be possible to measure colors to a thousandth of a magnitude, for bright stars. However, the color zero-points then

^{14b} J. D. Forbes, *Phil. Trans.* **132**, 225 (1842).

[†] Abbot *et al.*^{12a} (p. 344) arrived at the same conclusion: "On account of the uncertainty which attends the theory of the determination of air masses, when zenith distances exceeding 75° are in question, we conceive that it will be better to confine our observations... to the range of air masses less than 4..." Similarly, Forbes (Ref. 14b, p. 235) remarks that "...we would do well to avoid much use of observations near the horizon... any law of extinction will, therefore, be better determined from multiplied observations at elevations above 15° , than by those nearer the horizon..." Both of these authors stress the importance of adhering to the region where the simple $\sec z$ approximation is adequate.

depend on gain drifts between different photomultipliers, and must be controlled by using a broad-band standard source with good spectral stability (not a phosphor source). If a single photomultiplier is used with filters, one must observe in forward and then in backward sequence through the filters, and then interpolate all colors to a common time. This is inconvenient if more than 3 or 4 filters are used; furthermore, some efficiency is lost if gain changes are required in going from one filter to another, because all changes must be made twice. If many filters are used, linear interpolation between two deflections several minutes apart may not be adequate at the large air masses.

In *UBV* photometry, it is customary to measure in the order (*B*, *V*, *U*, red leak) to keep most gain changes unidirectional. The *B* and *U* deflections typically differ by about 1 min in time. Figure 13 shows the air-mass change in 1 min for several common situations, as a function of air mass. At moderate air masses, the change amounts to several hundredths of an air mass. This is already an important effect, but we know

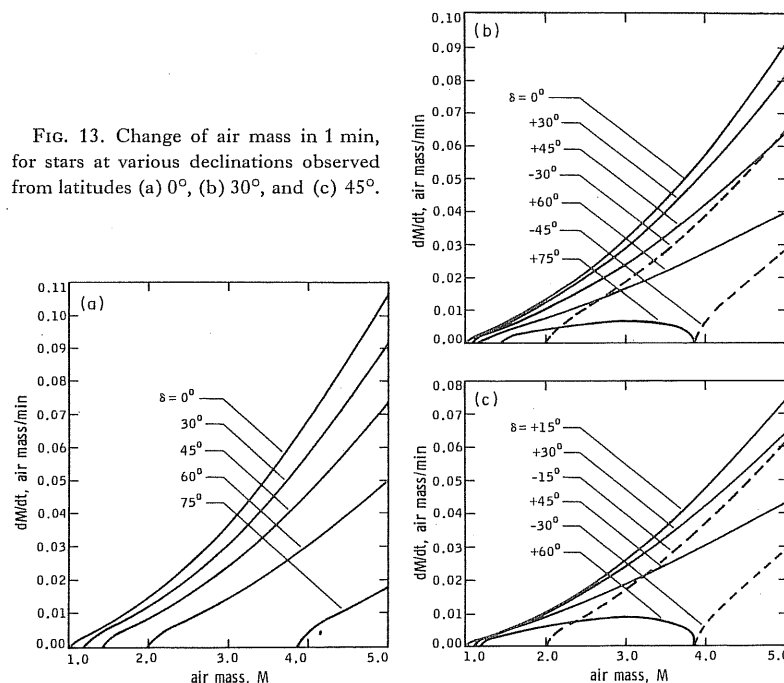


FIG. 13. Change of air mass in 1 min, for stars at various declinations observed from latitudes (a) 0° , (b) 30° , and (c) 45° .

of one instance in which very faint objects were observed, so that long integrations were necessary, together with equally long sky measurements. In this case, 10 min or more were spent on each filter, and the systematic errors that resulted from reducing "colors" instead of magnitudes sometimes exceeded a tenth of a magnitude! The same problem arises in spectrum scanning, where 10–20 min may be required for a complete scan. In such cases, it is essential to use the correct air mass for each color, as was done in the program described by Young and Irvine.^{7a} Of course, beyond about $\sec z = 3$, even simultaneous observations in different colors can have significantly different air masses (see Fig. 11).

One supposed advantage of using colors instead of magnitudes is that the instrumental color zero points are more stable than the magnitude zero. However, in fact, the colors are typically¹⁵ more stable by a factor of only 2 or 3, and the variations should in any case be measured and removed with a reliable standard source. Thus this argument works only for uncontrolled, unstable instruments. If the instrument is stable, individual magnitudes should be more precise than their differences (colors) by a factor of $2^{1/2}$, except in the important case of simultaneous measurements where cancellation of scintillation noise is possible.

Another argument is that the variations in extinction are strongly correlated in neighboring colors, so that the extinction coefficients for colors vary less than for magnitudes. Granted; but so what? If, say, an ultraviolet magnitude is needed, the sum of the small errors in V , $B - V$, and $U - B$ is the same as the original error in the U magnitude; alternatively, if colors are wanted, the (correlated) magnitude errors are just as diminished by differencing after extinction correction as before, provided that the correction is accurate. Thus the results should be the same whether the data are reduced as magnitudes or as colors.

The choice whether to reduce magnitudes or colors therefore depends primarily on (1) the quality and type of the instrumentation, and (2) the way in which observations in different colors are disposed in time—sequentially, symmetrically, or simultaneously. Good results can be obtained only if the reduction program is appropriate to the data at hand.

The second class of color problems has to do with bandwidth effects. Within each filter passband, some wavelengths suffer more extinction than others. Thus some stars (generally, bluer ones) suffer more extinction than others. Furthermore, at greater air masses the more susceptible rays are more completely removed, so that the incremental ex-

inction per air mass becomes less and less (the Forbes^{14b} effect); in modern terms, this is a curve-of-growth phenomenon. These problems were treated theoretically by King¹⁶ twenty years ago, but the theory is generally ignored. Instead, it is customary to represent the extinction by a formula like

$$m = m_0 + (A_0 + A_1 C) \cdot M, \quad (3.1.44)$$

where m may be either a magnitude or a color, C is a color, and M is the air mass.

To see how this is related to King's theory,¹⁶ we rewrite King's Eq. (21) for the extinction as

$$\Delta m = 0.543 w^2 \left(\lambda^2 \frac{I''}{I} \right)_0 - \left\{ 1 + \frac{n(n+1)}{2} w^2 - n N w^2 \right\} A_0 M + \frac{n^2}{2.17} w^2 (A_0 M)^2, \quad (3.1.45)$$

where primes denote wavelength derivatives; the zero subscript refers to evaluations at the effective wavelength λ_0 ;

$$w = \mu_2 / \lambda_0 \quad (3.1.46)$$

is the normalized (rms fractional) bandwidth defined by King's Eq. (8);

$$n = -(d \ln A / d \ln \lambda)_0 \quad (3.1.47)$$

is (minus) the logarithmic gradient of the monochromatic extinction $A(\lambda)$ at λ_0 ;

$$N = (d \ln I / d \ln \lambda)_0 \quad (3.1.48)$$

is the logarithmic gradient of the star's spectrum $I(\lambda)$ at λ_0 ; and $M \approx \sec z$ is the air mass. Thus, n and N represent the atmospheric reddening and the color of the star, respectively. As King points out, the first term is the color equation between monochromatic and wideband magnitudes at λ_0 , and can be dropped. We then have

$$\Delta m = M \{ A_0 [1 + w^2 n(n+1)/2] - w^2 n A_0 [N + (n/2.17) A_0 M] \}. \quad (3.1.49)$$

Now, w^2 is 0.007 for B and 0.004 for V ; and n is at most 4, for pure Rayleigh scattering, so that $n(n+1)/2 \leq 10$. Thus, the second term in

¹⁵ A. T. Young, *Mon. Notices Roy. Astron. Soc.* **135**, 175 (1967).

¹⁶ Ivan King, *Astron. J.* **57**, 253 (1952).

the first square brackets is, at most, 0.07, and usually much smaller. [Notice that its effect is to produce a shift in the effective wavelength at which the extinction is measured; it plays a role, with respect to the extinction, similar to that played by King's dropped term in $(\lambda^2 I''/I)$, with respect to magnitudes.] We need not drop this term, if we write

$$A_0^* = A_0[1 + w^2 n(n+1)/2]. \quad (3.1.50)$$

We now have the problem of expressing n and N in terms of measurable quantities. To do this, suppose that we have measurements in a *second* band centered at $\lambda_1 < \lambda_0$, but nearby λ_0 . (We suppose $\lambda_1 < \lambda_0$ for definiteness in the choice of signs; the opposite inequality could also be used for the derivation.)

We now approximate the required logarithmic derivatives by finite differences, a procedure that should not be far wrong if λ_1 is not far from λ_0 :

$$N = \frac{d(\ln I)}{d(\ln \lambda)} = \frac{d(\log I)}{d(\log \lambda)} \approx \frac{\log(I_0/I_1)}{\log(\lambda_0/\lambda_1)} = \frac{0.4(m_1 - m_0)}{\log(\lambda_0/\lambda_1)}, \quad (3.1.51a)$$

or

$$N = 0.4 \Delta X / \log(\lambda_0/\lambda_1) \quad (3.1.51b)$$

in the notation of Young and Irvine;^{7a} ΔX is the star's extra-atmospheric color index.

Similarly,

$$\begin{aligned} n &= \frac{-d(\ln A)}{d(\ln \lambda)} = \frac{-\lambda_0}{A_0} \left(\frac{dA}{d\lambda} \right)_0 \approx \frac{-\lambda_0}{A_0} \left(\frac{A_0 - A_1}{\lambda_0 - \lambda_1} \right) \\ &= \frac{\lambda_0}{(\lambda_0 - \lambda_1)} \cdot \frac{(A_1 - A_0)}{A_0} = \frac{\lambda_0}{(\lambda_0 - \lambda_1)} \cdot \left(\frac{\Delta A}{A_0} \right). \end{aligned} \quad (3.1.52)$$

[Notice that in both ΔX and ΔA the shorter-wavelength item comes first, so that red stars have positive (ΔX) colors and N , and a reddening atmosphere has positive ΔA and n .]

Now we use these approximations in Eq. (3.1.49):

$$\begin{aligned} \Delta m &= M \left\{ A_0^* - \frac{w^2 A_0 \lambda_0 \Delta A}{(\lambda_0 - \lambda_1) A_0} \left[\frac{0.4 \Delta X}{\log(\lambda_0/\lambda_1)} + \frac{\lambda_0 \Delta A}{2.17(\lambda_0 - \lambda_1) A_0} \cdot A_0 M \right] \right\} \\ &= M \left\{ A_0^* - w^2 \frac{\lambda_0}{(\lambda_0 - \lambda_1)} \left[\frac{0.4}{\log(\lambda_0/\lambda_1)} \right] \right. \\ &\quad \left. \times \Delta A \left[\Delta X + \frac{\lambda_0 \log(\lambda_0/\lambda_1)}{0.868(\lambda_0 - \lambda_1)} (\Delta A) M \right] \right\}. \end{aligned} \quad (3.1.53)$$

Let us call

$$\frac{0.4w^2 \lambda_0}{(\lambda_0 - \lambda_1) \log(\lambda_0/\lambda_1)} = W. \quad (3.1.54)$$

We can simplify these last two equations by converting $\log_{10}(\lambda_0/\lambda_1)$ to $\ln(\lambda_0/\lambda_1)$ and expanding, using the assumption that $(\lambda_0 - \lambda_1) \ll \lambda_0$:

$$\begin{aligned} \log\left(\frac{\lambda_0}{\lambda_1}\right) &= (\log_{10} e) \ln\left(\frac{\lambda_0}{\lambda_1}\right) = 0.434 \ln\left[1 + \frac{(\lambda_0 - \lambda_1)}{\lambda_1}\right] \\ &\approx 0.434 \left[\frac{\lambda_0 - \lambda_1}{\lambda_1} \right] \approx 0.434 \left[\frac{\lambda_0 - \lambda_1}{\lambda_0} \right]. \end{aligned} \quad (3.1.55)$$

Then, to this degree of approximation,

$$W \approx \frac{0.4w^2}{0.434} \left(\frac{\lambda_0}{\lambda_0 - \lambda_1} \right)^2 = \frac{w^2}{1.086} \left(\frac{\lambda_0}{\lambda_0 - \lambda_1} \right)^2, \quad (3.1.56)$$

and Eq. (3.1.53) becomes

$$\Delta m = M \{ A_0^* - W \cdot \Delta A [\Delta X + M \Delta A / 2] \}. \quad (3.1.57)$$

As a practical matter, we must employ the approximation $\Delta A \approx \Delta A^* = A_1^* - A_0^*$; if we drop the subscripts and superscripts, this is Eq. (4) of Young and Irvine.^{7a} Comparison with the commonly used Eq. (3.1.44) shows that (setting $C = \Delta X$) the latter ignores both the Forbes effect [represented by the last term in Eq. (3.1.57)] and variations in atmospheric reddening (i.e., $W \cdot \Delta A$ is treated as a constant A_1).

There have been arguments as to whether the color C in Eq. (3.1.44) should be the observed or the extra-atmospheric color of the star; the foregoing linear theory shows that the *mean* of these should be used, to represent the Forbes effect properly. Figure 14 shows the results of a numerical experiment to test this idea. (The figure is similar to Fig. 1 of Hardie.¹⁷) The energy distributions of a number of stars were multiplied by typical instrumental response functions for the B and V bands, both without any atmospheric extinction, and with various amounts of extinction corresponding to 1.0, 1.5, ..., 5.0 air masses for a standard atmospheric extinction model.^{14a} The integrated responses were converted to magnitudes, and the total extinction computed as the magnitude difference between the value for M air masses and the extra-atmospheric value. The effective extinction coefficient (the ordinate in Fig. 14) was then computed as the ratio of the total extinction to the total air mass M . Thus, for each star there are nine extinction values, which are plotted

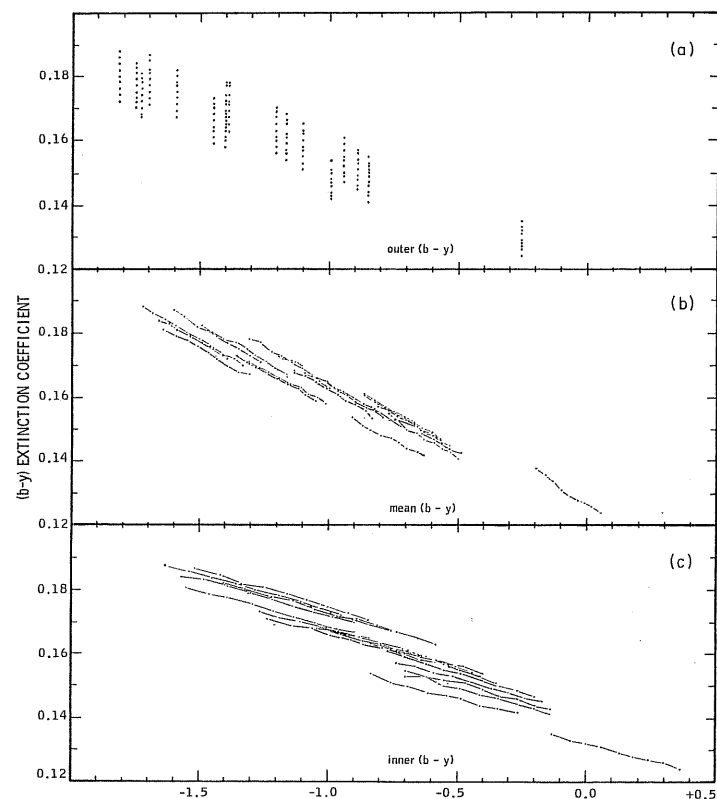


FIG. 14. Effective extinction coefficient (mag/air mass) found from numerical integrations, as a function of (a) extra-atmospheric color of star; (c) observed color; and (b) mean color (see text for explanation).

as a function of the instrumental color outside the atmosphere (a); the apparent color inside the atmosphere, at M air masses (c); and the mean of these two colors (b). In the latter two cases, successive "observations" of each star at different air masses are joined by a straight line. The mean color gives the best results, both in terms of minimum dispersion about the mean relation and also in the sense that it gives each star an atmospheric "reddening line" most nearly parallel to the general relation for all stars together, which means that the extrapolated extra-atmospheric value for a star is independent of the air mass at which it was observed. Notice, however, that there is some intrinsic spread between different

stars; i.e., two stars can have the same color but different extinction coefficients. This is due to two factors: (1) higher-order terms, omitted from the theory; and (2) an imperfect correlation between $(b - y)$ color and the spectral gradients at the effective wavelengths of the bands, owing to blanketing, rotation, microturbulence, and other effects. (Similar results were found for other colors and magnitudes.)

The Forbes effect is appreciable, especially in the ultraviolet magnitude. Figure 15 shows extinction curves from the numerical integrations, together with Hardie's observations.¹⁷ Most of the curvature of the extinction lines occurs at *small* air masses, which explains why Hardie's data do not show the effect between 2 and 6 air masses. This is due to the increasing monochromaticity at large air masses, after the shorter

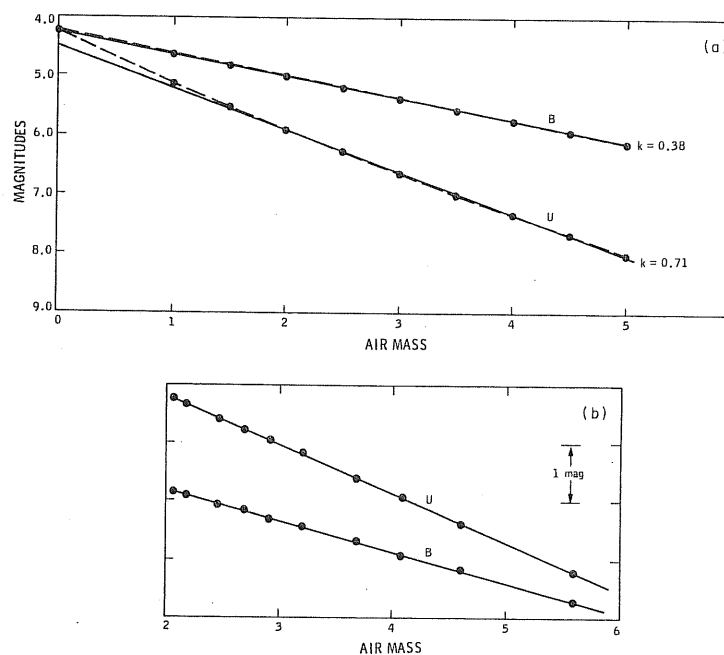


FIG. 15. (a) Extinction curves (dashed) calculated from numerical integrations for a B3 star. The solid straight lines are drawn to fit the points between 2 and 5 air masses; (b) Hardie's observed extinction curves at low altitudes for π^2 Ori.

¹⁷ R. H. Hardie, in "Spectral Classification and Multicolour Photometry," p. 243. IAU Symp. No. 24 held in Saltsjöbaden, Sweden, 17-21 August 1964. Academic Press, New York, 1966.

wavelengths have been almost completely removed. However, as can be seen from the figure, the straight line fit to the 2–5 air-mass region gives systematic errors in the extrapolated extra-atmospheric magnitudes of 0.03 mag in B , and about 0.25 mag in U . A straight line passed through the calculated points at 2.0 and 5.0 air masses misses the point at $M = 3.5$ by only 0.008 mag in B and 0.034 mag in U , which corresponds to air-mass errors of 0.02 and 0.05 in B and U , respectively. The rms residual from a linear least-squares fit would be less than a hundredth of a magnitude for both colors in this region. Thus, although a straight line is an excellent representation of the large-air-mass data, it involves large errors in extrapolating to zero air mass.

With respect to the parameters W and w^2 , we might add that for B and V , $\lambda_0/\Delta\lambda$ is about 5 or 6; then $W \approx 30w^2$. King gives $w^2 = 0.007$ for B and 0.004 for V , based on rather poor values of the response functions; the problem is further complicated by the Chappuis bands of ozone, which greatly reduce the effective value of n across the V band. Anyway, one might expect $W \approx 0.21$ or so for B , and something less than 0.12 for V . Our Agassiz Station reductions give $W_B = 0.26$ fairly consistently, and $W_V \approx 0.03$; the numerically integrated values were reduced, using a program based on this theory,^{7a} and gave $W_B = 0.21$, $W_V = 0.026$. (One effect of the ozone is to make the extinction larger in V , which reduces the apparent ($B - V$) extinction gradient below its true value across the B band, so it is not surprising that W_B comes out a bit larger than expected.)

In common practice, the parameter A_1 in Eq. (3.1.44) is generally assumed to be either a free parameter that is solved for separately on each night, or a fixed constant whose value is found once for all time. However, the theory [Eq. (3.1.57)] shows that it should depend on the reddening power of the atmosphere ΔA . If the parameter A_1 is free, it can soak up and conceal various systematic errors. On the other hand, if it is fixed, it introduces systematic errors in the results whenever the atmospheric extinction law changes (due to seasonal or random effects such as volcanic eruptions¹⁸). If the variable part of the extinction were neutral, ΔA would be constant; but it is not, as the variable color of the setting sun vividly demonstrates. Only by making the mathematical representation of extinction conform to the physical situation can we hope to obtain accurate results.

A computer program that does represent the color terms according to

¹⁸ G. de Vaucouleurs, *Publ. Astron. Soc. Pacific* 77, 5 (1965).

this theory has been used and described by Young and Irvine.^{7a} The added complexity of using a correct representation of the physics of extinction is so small, compared to the capabilities of modern computers, that simplicity is no longer an acceptable excuse for inaccurate results. One must bear in mind that an incorrectly formulated least-squares program will absorb systematic errors into whatever adjustable parameters it has available. Thus, particularly if there are only a few observations for each disposable parameter, systematically wrong values will be found that may fit the data quite well. Small residuals (high precision) do not mean small errors (high accuracy).

3.1.5.2. Errors Due to Misuse of Least Squares. It should be remembered that the expectation values of the parameters in a least-squares solution are their true values only if certain assumptions are satisfied. In particular, the errors in the observations are supposed to be normally distributed, with mean zero. If the resulting estimate is to be efficient, the equations of condition must be weighted, so that the residuals are all drawn from the same parent population (i.e., they must all have the same probable error). These conditions are often violated in practice.

First of all, the observed quantities are intensities, not magnitudes. In the presence of any experimental error, the mean intensity does not correspond to the mean magnitude, because the logarithm of the mean of a random variable is not equal to the mean of its logarithm. It is clear from the law of conservation of energy that scintillation can redistribute the energy in the shadow pattern, but cannot alter the mean intensity. In fact, it is well known that scintillation causes the logarithm of the intensity (i.e., magnitudes) to be normally distributed, and that in this case the difference in the means is

$$\log\langle I \rangle - \langle \log I \rangle = \sigma^2/2, \quad (3.1.58)$$

where the angular brackets denote averaging, and σ^2 is the variance of $\log I$. Natural logarithms are close enough to magnitudes that we can also consider σ^2 to be the variance of the magnitude estimates. For example, if $\sigma_m = 0.1$ mag, Eq. (3.1.58) tells us that the mean magnitude differs from the true magnitude of the star by 0.005 mag, which begins to be important. This sets a practical lower limit to the duration of photometric observations. For example, if we wish to use a 40-cm (16-in.) telescope at 3 air masses, Table I of Part 2 shows that about a 10-sec integration is required to achieve rms errors of 0.01 mag on bright stars,

which means significant systematic errors will appear if integrations shorter than 0.1 sec are used.

At the other extreme, the errors on faint stars are dominated by photon noise and sky noise, which may easily exceed 0.1 mag. Furthermore, these errors are not distributed normally (or even symmetrically) in magnitude, which leads to further systematic errors. It appears that the photometrist's only hope in such cases is to observe faint stars only near the meridian, so that a long enough integration can be achieved to reduce the random (and consequent systematic) errors to an acceptable level, while keeping the air mass practically constant. Otherwise, the whole quasi-linear system of equations using magnitudes must be replaced by a system of (exponential!) equations in terms of intensities. Without such precautions, the mean magnitudes will depart more and more from a Pogson scale at the faint end. For example, adding 30% to the intensity decreases its magnitude by 0.29, but subtracting 30% increases the magnitude by 0.39; the mean intensity is correct, but the mean magnitude is 0.05 too faint. Again, the systematic error rises with the square of the noise level.

Finally, there is the question of weighting the observations. Because of the rapid increase in errors with $\sec z$, low-altitude observations have very low weight. For example, if the errors increase like $(\sec z)^2$, the weight of an observation is proportional to $(\sec z)^{-4}$. Thus, at two air masses, we have only 0.06 of the weight of a zenith star; at three, the weight is down to 0.012. These observations provide information about the extinction, but are worthless for determining the actual brightness of a star. Even at $z = 45^\circ$, the weight is down by a factor of four. Clearly, it is essential that a realistic weighting system be used, and that all program stars be observed as near the meridian as possible.

3.1.5.3. Errors Due to "Standard" Stars. Hardie^{4,19} has advocated the use of standard stars, whose extra-atmospheric values on the instrumental system are known, for quick measurements of the extinction. This works beautifully *if* these values are accurately known. Both the extinction and the instrumental magnitudes are determined simultaneously from many nights' data in the method of Young and Irvine,^{7a} and this is also satisfactory. A similar method has been used by Rufener,⁹ by Weaver,²⁰ and others.

¹⁹ R. H. Hardie, *Astrophys. J.* **130**, 663 (1959).

²⁰ H. F. Weaver, *Astrophys. J.* **116**, 612 (1952).

However, some observers have relied on the *published* magnitudes of *UBV* standard stars, rather than determining good instrumental values themselves. They then solve for the transformation coefficients between instrumental and standard systems, as well as for the extinction coefficients. Unfortunately, the *UBV* "standards" contain mean errors per star on the order of 0.02 mag; furthermore, the usual linear transformations are imperfect, especially in the ultraviolet, and may contribute similar errors of a systematic nature. If a large number of standard stars were observed, their errors should average out. (For example, Johnson and Harris⁵ say that "it is best . . . to use at least 20 stars of all types . . .") However, the standard stars are usually regarded as a "shortcut" to extinction; we have seen as few as four or five stars used altogether. In such cases, the *accidental* errors in the published values for the particular stars used become appreciable *systematic* errors in the extinction and the transformation coefficients, and consequently in the final results. Recently, Moreno⁶ has shown that the errors introduced by incorrect extinction coefficients are not transformed away by adjusting the transformation coefficients. Here again is a situation in which the least-squares process absorbs systematic effects, producing small internal but large external errors.

3.1.6. Actual Error Laws

From the foregoing discussion, it is clear that unavoidable systematic errors that depend on variable atmospheric conditions (seeing; vertical distribution of absorbers) become important in the neighborhood of 3 or 4 air masses, so that larger air masses should be avoided in work of the best quality. Within this range, it is still important to know how the random errors actually vary with air mass; not only to plan observations for maximum efficiency, but also to assign realistic weights in reducing the data.

Very few observers have bothered to investigate their errors as a function of air mass. Rufener⁹ has given a very thorough discussion of errors in the Geneva photometry. His errors due to scintillation (from his Fig. 9) are replotted in log-log coordinates in Fig. 16. The lines, which have been drawn by eye to fit these data, have very nearly slope 2; that is, the scintillation errors grow like $(\sec z)^2$, as expected. In addition, he finds a root mean square fixed error of about 0.006 mag, due to instrumental uncertainties (mainly due to nonlinearity, and gain changes). These appear to be the principal sources of error in determining the

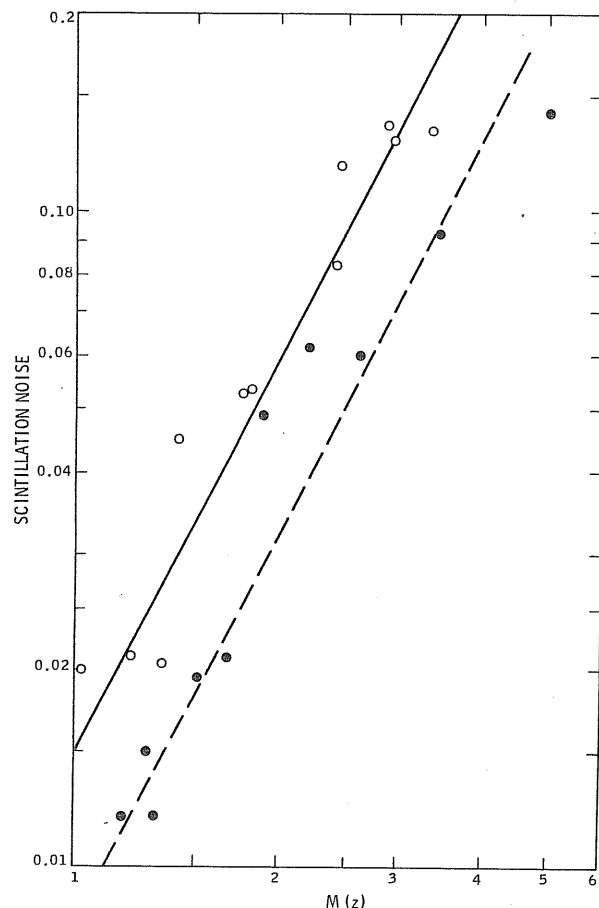


FIG. 16. Scintillation noise at Geneva, in units of $\Delta d/d$, on nights of strong (open circles and upper curve) and weak (filled circles and lower curve) scintillation [taken from Fig. 9 of F. Rufener, *Publ. Obs. Geneve, Ser. A.* No. 66 (1964)].

extinction at Geneva, apart from time variations of the extinction coefficient, which are carefully monitored. Evidently the scintillation noise dominates.

Another example of careful work is given by Stock,²¹ who also found the errors to increase with the square of the airmass, and derived from

²¹ J. Stock, *Vistas Astron.* 11, 127 (1968).

this the condition $M_2 = 2.1$ [as pointed out in the discussion following Eq. (3.1.8)].

We had also come to this conclusion at about the same time;²² a slide of Fig. 1 was shown at the December, 1966, AAS meeting. Immediately afterward, Hardie told us that he had found a contrary result experimentally: the extinction was most precisely determined for very large values of M_2 , rather than showing an optimum near 2 or 3 air masses. We now believe this is due to Hardie's method of determining the extinction by using the published values of UBV for standard stars. For, in this case, the (constant) errors in the standards themselves are dominant at small-to-moderate air masses, so that $p \approx 0$ (cf., Fig. 1). The effective error law would then consist of this large constant term, in addition to the usual $(\sec z)^2$ term for scintillation. The weighting scheme used in determining the extinction should reflect the effect of this constant error term; however, observations of bright *program* stars should still receive the $(\sec z)^{-4}$ weights appropriate to scintillation noise alone.

As a final example, Fig. 17 shows estimates of the error law from data taken at Agassiz Station and reduced with the program described previously.^{7a} The original data were taken in pairs of 20-sec deflections; but because the efficiency of reading the chart paper is only³⁰ about 25%, the scintillation noise should be that for a 10-sec deflection, which is 0.001 mag at the zenith for a 60-cm (24-in.) telescope (see Part 2, Table I). The root mean square residual, expressed in magnitudes, was computed for data grouped into four intervals of air mass: 1.0–1.2, 1.2–1.5, 1.5–2.0, and 2.0–3.0; only stars observed five or more times were used, so that errors in their instrumental magnitudes should not strongly affect the results. Also, only nights with no marked systematic run of residuals were used. The December, 1960, data show rather large errors, roughly proportional to air mass. This suggests that small variations in the extinction coefficient with time were the main source of error, a conclusion supported by considerable systematic runs in the residuals on about half the nights of that month. On the other hand, the March 1961 data are much better, although they are still far above the level of pure scintillation noise. A constant error of about 0.007 mag seems to dominate these observations at small air masses.

As a practical matter, the above studies suggest that, under good conditions, the error law can be approximately represented by a combination of constant and scintillation errors. Of course, the scintillation

²² A. T. Young, *Astron. J.* 72, 328 (1967).

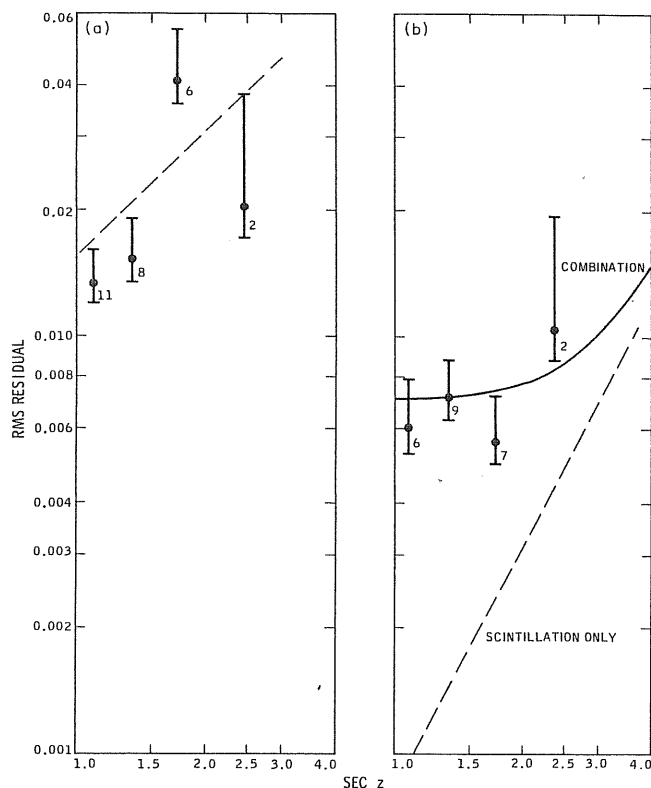


FIG. 17. rms errors in V magnitude vs. air mass, for two periods at Agassiz Station. The data were taken with the 60-cm (24-in.) Clark reflector. (a) December, 1960. The errors are large, and increase roughly proportionally to the air mass, as indicated by the dashed line. (b) March 1961. The errors are smaller, and seem to be composed of a constant component (~ 0.007) plus scintillation (shown by the dashed line); the heavy curve is the combination of these terms. (The "error bars" represent 50% confidence intervals.) The number of observations included in each point is indicated beside the "error bar."

component may be negligible for large apertures (say, over 150 cm); but most photometry is done with smaller instruments. However, regardless of the shape of the random error law, its dependence on air mass can be found from the observations. Then, given the actual error law, how can we find the optimum air mass for extinction measurement?

Let the random error law be some function $\sigma(M)$, which may be given

numerically or graphically. In the simplest case, Eq. (3.1.4) tells us that variance in the extinction coefficient derived from two observations at M_1 and M_2 is just

$$\sigma_A^2 = [\sigma^2(M_1) + \sigma^2(M_2)] / (M_2 - M_1)^2. \quad (3.1.59)$$

This suggests a simple graphical method of finding the optimum M_2 : if we pick a value of M_1 and plot the function $\sigma^2(M_2)$ as a function of $(M_2 - M_1)^2$, then the tangent to this curve from the point $[-\sigma^2(M_1), M_1]$ has the least slope (σ_A^2) of all lines from that point to the curve (see Fig.

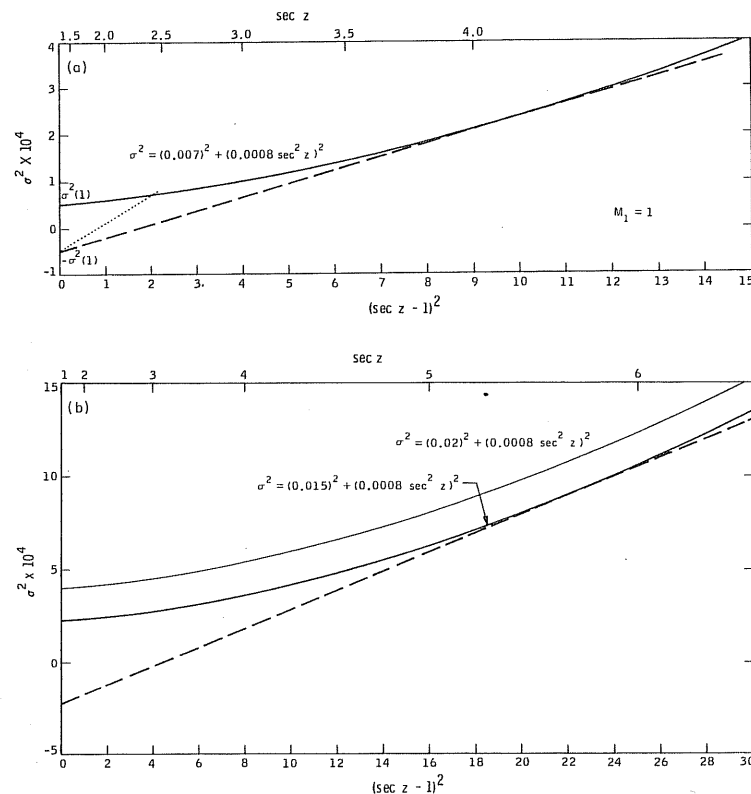


FIG. 18. Graphical determination of optimum air mass for extinction determination. (a) Error law (solid curve) taken from curve of Fig. 17b. Dashed line: determination of optimum M_2 . Dotted line: determination of half-optimum M_2 . (b) Same scintillation noise as (a), but with constant errors of 0.015 and 0.020 mag. (The dashed line picks out $M_2 \approx 6$ for the former.)

18). Therefore the value of M_2 at the point of tangency is the optimum value. Furthermore, any chord drawn from the specified point intersects the curve in two points, such that their values of M_2 give equally good determinations of the extinction coefficient (apart from systematic errors, of course).

For example, Fig. 18a shows the error law found for the March, 1961, observations of Fig. 17. If we take $M_1 = 1$, the zenith variance is about 5×10^{-5} (mag)². The (dashed) tangent to the curve from the point $-\sigma^2 = -5 \times 10^{-5}$, on the vertical axis, meets the curve at about $M_2 = 4.1$. If we draw a line from the same point, but with twice the slope (i.e., twice the value of σ_{A^2}), we find it meets the curve at $M_2 \approx 2.4$; thus the extinction is determined with half the optimum weight, or $2^{1/2}$ times the minimum error, if we use $M_2 = 2.4$.

What would be the situation if we had used the *UBV* standard magnitudes, linearly transformed to the instrumental system? In fact, the transformation between *V* and the instrumental magnitude left a root mean square residual of 0.015 mag per star, which is clearly much larger than the internal errors of the March photometry (especially considering that the standard stars were observed an average of 4 times apiece in this run). Whether this 0.015-mag error is due to the errors in the tabulated values, or to transformation errors, is immaterial for our present purposes; in either case, it acts like a constant error if the published values are used to determine the extinction. The effect of increasing the constant error from 0.007 to 0.015 mag is shown by Fig. 18b; the optimum air mass M_2 has increased to about 6. In general, the situation will be still worse, as the March observations use only the brightest and best-determined of the *UBV* standards. If the constant error is raised to the more typical 0.02 mag for run-of-the-mill *UBV* standards, M_2 becomes very large indeed—in agreement with Hardie's statement, and in spite of the rapid increase in scintillation with air mass.

In case we do not spend equal amounts of time at the high and low air masses, Eq. (3.1.12) shows us how to modify the graph. If we multiply through by f , we obtain

$$f\sigma_{A^2} = \frac{1}{n(M_2 - M_1)^2} \left[\frac{f}{(1-f)} \sigma^2(M_1) + \sigma^2(M_2) \right]. \quad (3.1.60)$$

Notice that the term in $\sigma^2(M_1)$ contains a factor $[f/(1-f)]$, which is the ratio of the observing time spent at M_2 to that spent at M_1 . For example, if we observe a star at M_2 , both rising and setting, as well as at M_1 , on the meridian, the factor is 2. Then to find the optimum M_2 ,

we must draw the tangent from the point $-2\sigma^2(M_1)$ instead of just $-\sigma^2(M_1)$. In general, we simply move the pivot point down by a factor equal to the ratio of the observing times. As is evident from the shape of the curves in Fig. 18, increasing this ratio also increases the optimum value of M_2 . (This can also be seen from the shapes of the contours in Figs. 3 and 4.)

3.1.7. How Much Time to Spend on Extinction

3.1.7.1. General Principles. Because the errors in the extinction observations propagate through the extinction corrections into the final results, enough effort must be spent in determining the extinction to guarantee adequate precision and accuracy. However, how much is "enough"? The answer obviously depends on the type of work being done.

In general, the variance in a magnitude or color, after correction for extinction, will be

$$\sigma^2 = \sigma_{\text{obs}}^2 + \sigma_{\text{ext}}^2 + \sigma_z^2, \quad (3.1.61)$$

where σ_{obs}^2 is the variance due to observational errors of the program star itself, σ_{ext}^2 is the variance propagated from extinction errors, and σ_z^2 is the zero-point variance. If each night is reduced separately, or if the zero point is allowed to be a free parameter for each night, the first two terms on the right correspond roughly to the "internal error," and the whole expression is the "external error." The separation of σ_{ext} and σ_z is somewhat artificial, as they usually depend on the same observations, so these errors are not always independent, as assumed in Eq. (3.1.61).

In order to keep σ_{obs}^2 small, we usually observe the program star near its minimum zenith distance M^* , and reobserve it several times; then

$$\sigma_{\text{obs}}^2 \approx \sigma^2(M^*)/n, \quad (3.1.62)$$

if we have n observations altogether. In good conditions, small values of n (say 2 or 3) suffice to reduce σ_{obs} to a few thousandths of a magnitude.

The contribution of the extinction errors is more complicated to assess, because extinction stars are usually standard (zero-point) stars as well. Thus we must consider the techniques used to collect and reduce the data, as well as the ultimate use to which the results are put.

3.1.7.2. Absolute Photometry. If we are doing absolute photometry (comparing a star to a standard lamp), then

$$\sigma_{\text{ext}} = M^* \cdot \sigma_A; \quad (3.1.63)$$

and as M^* must exceed unity, the error σ_A in the extinction coefficient appears with full force. It is not always realized that this same large error appears whenever we assume that some instrumental zero point remains constant from night to night, as is often done in the case of colors.^{4,7a,20} The assumption of a fixed zero point (which can be ensured only by using a reliable standard source) greatly strengthens the precision of extinction determination when data from different nights are combined; however, if it is not strictly true, it can introduce considerable systematic errors. Thus, we achieve precision at the risk of accuracy.

3.1.7.3. Relative Photometry

3.1.7.3.1. PRINCIPLES. To avoid this problem, it is common practice to let the nightly zero points be free parameters. The determination of the zero point then depends on observations of certain (instrumental) standard stars. It is often claimed that this reduces the problem to relative photometry, so that the extinction errors cancel out. This implication is only partially true, however; if either the program or the standard stars are distributed over the sky, there will be an error of the form

$$\sigma_{\text{ext}}^2 = \overline{(\bar{M}_{\text{std}} - M^*)^2} \cdot \sigma_A^2 = \sigma_M^2 \cdot \sigma_A^2, \quad (3.1.64)$$

where the rms air-mass difference σ_M can hardly be less than several tenths.[†] Thus, compared to absolute photometry, the extinction error σ_{ext} in relative photometry is reduced only by a factor $(\bar{M}_{\text{std}} - M^*)_{\text{rms}}/M^*$, which is usually rather modest (say about $\frac{1}{3}$), and which may well be compensated by the increased uncertainty σ_A in the extinction itself, owing to the sparser distribution of observational degrees of freedom over the set of unknown parameters. Furthermore, it is clear that errors in the deduced nightly zero points appear in the results as systematic errors. Once again, the importance of matching the mathematical model to the physical situation is evident.

[†] Note that this error results from the *variance* in air mass, even if the *mean* air masses of extinction and program stars are the same.

3.1.7.3.2. DIFFERENTIAL PHOTOMETRY. Of the two factors on the right of Eq. (3.1.64), σ_A^2 can be found from the slope of a straight line in a diagram such as Fig. 18. The other factor (air-mass variance) deserves further attention. As is well known, it can be made very small by making all observations at nearly the same air mass, usually that of the Pole. A few reference stars near the Pole can then be used to measure and remove temporal changes in both extinction and instrumental zero point.

This practice is now less popular than it once was. Some telescopes are difficult (or even impossible) to use near the Pole. At high latitudes, the polar-altitude condition restricts observations to a small range of declination; at low latitudes, the polar altitude is so low that the observational errors (both σ_{obs} and σ_z) are offensively large. If some other reference altitude is used, the reference stars traverse an appreciable range of air mass during a night, so the extinction error becomes appreciable once again.

Another case in which the air-mass factor is very small is differential photometry of variable stars. Since a comparison star bright enough to be dominated by scintillation noise can usually be found within one or two tenths of a degree of the variable, the air-mass difference can usually be kept below 0.01, up to 2 or 3 air masses. Thus the extinction coefficient needs to be known only to about 0.1 mag/air mass in order to keep magnitude errors below 0.001 mag. However, color-dependent terms in the extinction can cause much larger errors, especially during eclipses of binaries having dissimilar components.

These cases, in which the σ_{ext} term in Eq. (3.1.61) can be made small, require us to look at the σ_z term to determine the proper balance between program and reference stars. If both are bright enough that photon noise is negligible, $\sigma_z^2 \approx \sigma^2(M)/n_{\text{ref}}$, where n_{ref} is the number of reference-star observations that can be combined. For example, if the extinction coefficient and the instrumental zero point are constant, widely separated reference observations can be combined; but if there are variations, we may have to compare each program-star deflection with just one adjacent reference observation. In the former (constant) case, we should observe the reference star the *same* number of times as each (constant) program star. For a variable star, each observation provides an independent point on the light curve, so $n_{\text{ref}} = 1$ will suffice, unless we are concerned about the systematic accuracy of placing the entire light curve on a standard system. In most cases, however, we have to worry about instrumental or extinction variations on the order of 0.01 mag/hr. Then $\sigma_z \sim 0.01 \Delta t$, where Δt is the time difference (in hours) between reference observations.

This is generally larger than σ_{obs} if Δt exceeds a few tenths of an hour. Thus, differential photometry usually requires several reference observations per hour, to achieve maximum precision.

If photon noise is important, the fainter star should receive most of the observing time. An argument like the derivation of Eq. (3.1.15) shows that, if the comparison star receives a fraction F of the total observing time, the program star is best determined if the ratio of the times devoted to the two stars is also the ratio of their standard errors for unit time, σ_c and σ_p , respectively:

$$F/(1 - F) = \sigma_c/\sigma_p, \quad (3.1.65)$$

or

$$F = \sigma_c/(\sigma_c + \sigma_p). \quad (3.1.66)$$

[Here, c and p denote "comparison" and "program" stars, respectively, and we have set $\sigma_{\text{obs}}^2 = \sigma_p^2(1 - F)^{-1}$, and $\sigma_z^2 = \sigma_c^2 F^{-1}$.]

In the case of pure photon noise, Eq. (3.1.65) is equal to $10^{0.2(m_c - m_p)}$; if the comparison star is so bright that photon noise is negligible, m_c should be replaced by the magnitude at which photon noise equals scintillation noise. Thus, a 15th mag program star should be observed ten times as long (or ten times as often, if each observation is of fixed length) as a 10th mag comparison star, to achieve the best measurement of their magnitude difference in a given amount of telescope time.

3.1.7.3.3. ALL-SKY PHOTOMETRY. Now let us consider observations over a considerable range of air mass, so that σ_{ext}^2 is appreciable. We must evaluate the air-mass variance factor in Eq. (3.1.64) to calculate this extinction error. Generally, each extinction star is observed at both large and small air mass, but each program star is observed only at its minimum air mass M^* . Also, the zero-point standard stars are usually used as extinction stars; this avoids the need for separate zero-point standards. Thus, the reference air mass \bar{M}_{std} in Eq. (3.1.64) is really \bar{M}_{ext} , the mean air mass of the extinction stars. This should be calculated using the appropriate (air-mass-dependent) weights, $1/\sigma^2(M)$, for lower and upper air masses:

$$\begin{aligned} \bar{M}_{\text{ext}} &= \left[\frac{(1-f)M_1}{\sigma^2(M_1)} + \frac{fM_2}{\sigma^2(M_2)} \right] \left[\frac{(1-f)}{\sigma^2(M_1)} + \frac{f}{\sigma^2(M_2)} \right]^{-1} \\ &= \frac{\sigma^2(M_2)(1-f)M_1 + \sigma^2(M_1)fM_2}{\sigma^2(M_2)(1-f) + \sigma^2(M_1)f}. \end{aligned} \quad (3.1.67)$$

Thus $\bar{M}_{\text{ext}} = (M_1 + M_2)/2$ only if $\sigma(M) = \text{constant}$, and $f = \frac{1}{2}$. If we

can assume $\sigma(M) \sim M^p$, Eq. (3.1.67) can be written as

$$\bar{M}_{\text{ext}} = M_1 \left[\frac{M_r^{2p} + f_r M_r}{M_r^{2p} + f_r} \right] = M_1 [1 + f_r(M_r - 1)(M_r^{2p} + f_r)^{-1}], \quad (3.1.68)$$

where

$$M_r = M_2/M_1 \quad (3.1.69)$$

is the ratio of the two air masses, and

$$f_r = f/(1 - f) \quad (3.1.70)$$

is the corresponding ratio of observing times.

For example, the common case of $M_1 = 1$, $f = \frac{2}{3}$, and $p = 2$ gives $M_2 \approx 2.2$ for optimum results; then $\bar{M}_{\text{ext}} = 1.1$. If $p = 1$ and $M_2 = 4$, we have $\bar{M}_{\text{ext}} = 1.33$. Evidently the higher weight of one zenith observation generally overcomes the greater number (f_r) of large-air-mass data, giving a mean air mass near M_1 .

On the other hand, even if program stars are observed only at culmination, many of them will be at considerably larger air masses. Their mean air mass can be roughly estimated by the following argument: suppose that program stars are uniformly distributed over the sky, and that they are observed only at culmination. Let us further suppose that only those stars culminating at $M^* \leq M_c$ are used. The uniform distribution means that the number of stars at declination δ is proportional to $\cos \delta$. If the observer's latitude is ϕ , stars culminate at $M^* = 1/\cos |\delta - \phi|$, assuming a flat earth. The cutoff M_c occurs at a declination

$$\delta_c = \phi - \cos^{-1}(1/M_c). \quad (3.1.71)$$

If we assume all stars poleward of δ_c are observed, including the small region near the pole where $M > M_c$ at low latitudes, we have

$$\begin{aligned} \bar{M}^* &= \int_{\delta_c}^{\pi/2} \cos \delta \sec(\delta - \phi) d\delta \Big/ \int_{\delta_c}^{\pi/2} \cos \delta d\delta \\ &= \frac{\left(\frac{\pi}{2} - \delta_c\right) \cos \phi - \sin \phi \left[\ln \frac{\cos(\phi - \delta_c)}{\sin \phi} \right]}{1 - \sin \delta_c}. \end{aligned} \quad (3.1.72)$$

Figure 19 shows the run of Eq. (3.1.72) with ϕ for several values of M_c . For moderate latitudes and M_c , $\bar{M} \approx 1.5$, which is a few tenths larger than typical values of \bar{M}_{ext} . In fact, the same argument can be used to

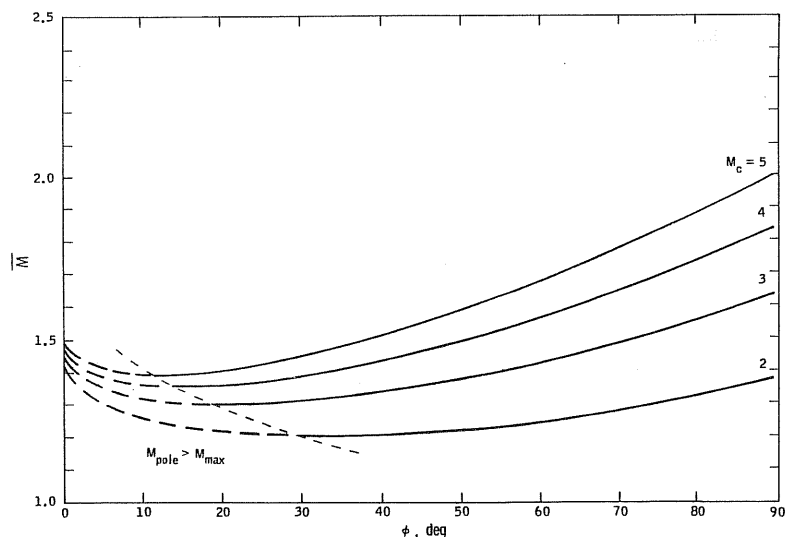


FIG. 19. Mean program-star air mass at culmination. Values of $\overline{M^*}$, estimated according to Eq. (3.1.72) for several values of M_c , as functions of the observer's latitude are shown. The dashed portions, to the left of the dotted curve, indicate the regions where $M > M_c$ near the Pole.

estimate the factor $\overline{(\overline{M}_{\text{ext}} - M^*)^2}$ that appears in Eq. (3.1.64). For,

$$\sigma_M^2 = \overline{(\overline{M}_{\text{ext}} - M^*)^2} = \overline{(\overline{M}_{\text{ext}})^2} - 2\overline{\overline{M}_{\text{ext}} M^*} + \overline{M^{*2}}, \quad (3.1.73)$$

where Eq. (3.1.72) gives $\overline{M^*}$, and

$$\begin{aligned} \overline{M^{*2}} &= \int_{\delta_c}^{\pi/2} \cos \delta \sec^2(\delta - \phi) d\delta \bigg/ \int_{\delta_c}^{\pi/2} \cos \delta d\delta \\ &= \frac{\left\{ \cos \phi \ln \left[\frac{\sec(\frac{1}{2}\pi - \phi) + \tan(\frac{1}{2}\pi - \phi)}{\sec(\delta_c - \phi) + \tan(\delta_c - \phi)} \right] \right\} \\ &\quad + \sin \phi [\sec(\delta_c - \phi) - \sec(\frac{1}{2}\pi - \phi)]}{1 - \sin \delta_c}. \end{aligned} \quad (3.1.74)$$

Figure 20 shows the course of Eq. (3.1.74) for the same values of M_c used in Fig. 19. These results allow the estimation of the air-mass variance factor by means of Eq. (3.1.73) if $\overline{M}_{\text{ext}}$ is specified. Figure 21 shows the results for $\overline{M}_{\text{ext}} = 1.1$ and 1.3, the typical values derived above.

As the values shown in Fig. 21 are several tenths at least, we can expect our program stars to have rms extinction-produced errors that are likewise several tenths of the error in the extinction coefficient, according to Eq.

(3.1.64). For example, a typical value of σ_M is about 0.4, if we are at a moderate latitude and avoid stars that transit within about 25° of the horizon. Then if σ_M , the standard error in the extinction coefficient, is 0.01 mag/air mass, the resulting rms program-star error will be 0.004 mag. This may be acceptable in some kinds of work; on the other hand, it is certainly larger than the random observational errors of the brighter program stars if an aperture over 40 cm (16 in.) is used (see Part 2, Table I). If a 90-cm (36-in.) telescope is used, this rms extinction error exceeds the photon noise for stars brighter than eleventh magnitude, for a 10-sec integration with B or V filter. Thus, if the final error caused

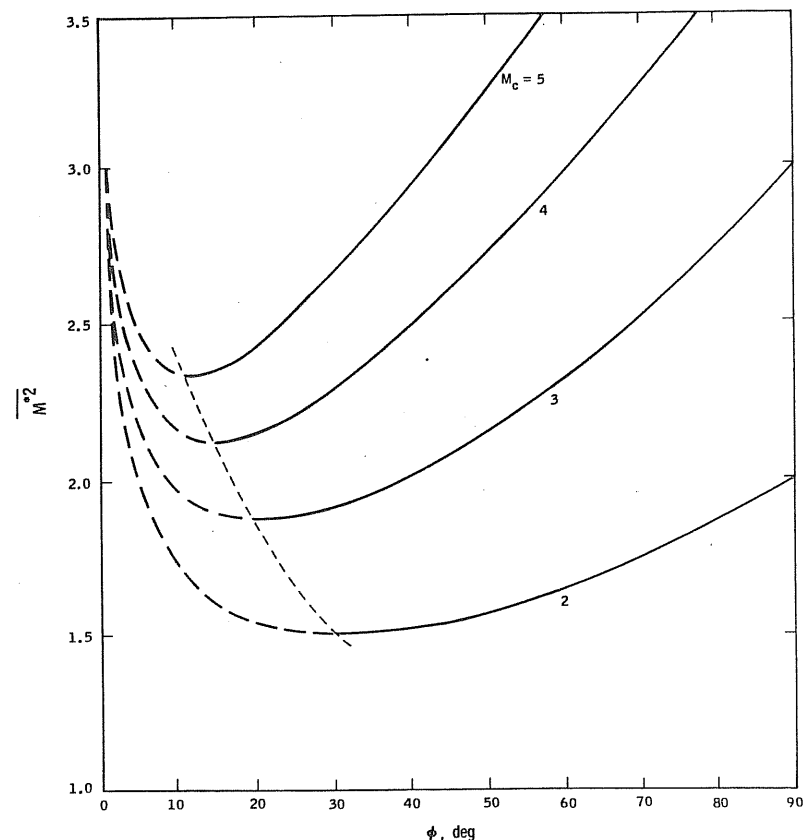


FIG. 20. Mean square program-star air mass $\overline{M^{*2}}$ at culmination, displayed as in Fig. 19.

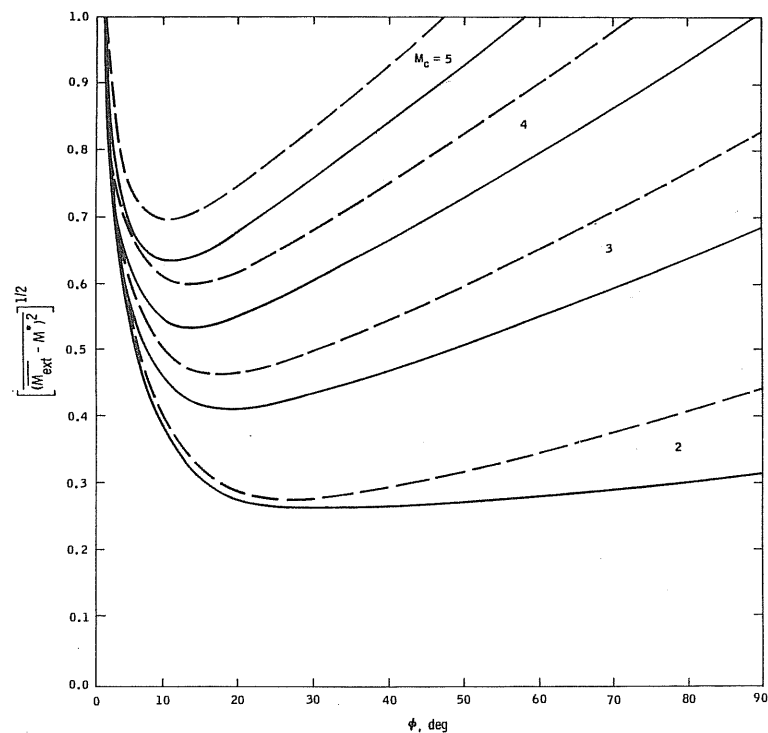


FIG. 21. The rms air-mass difference σ_M between program and extinction stars, for $\bar{M}_{\text{ext}} = 1.1$ (dashed) and 1.3 (solid curves), calculated from Eq. (3.1.73) in the text, with the help of Eqs. (3.1.72) and (3.1.74). As in Figs. 19 and 20, the large values at low latitudes are due to the polar region where $M > \bar{M}_c$.

by uncertainty in the extinction coefficient is to be kept smaller than the observational errors, we must generally know the extinction coefficient somewhat more precisely than 0.01 mag/air mass.

Let us again ask the question: what fraction F of the observing time should be devoted to extinction, to make optimum use of telescope time? (Again, suppose initially that only one program star is used.) Having determined our observational error law as a function of air mass, we can compute the error σ_1 to be expected from n_{ext} observations (suitably divided between M_1 and M_2) of an extinction star; for example, by using Eq. (3.1.12), or its graphical equivalent. Let us summarize this result as

$$\sigma_1^2 = \sigma_1^2/n_{\text{ext}}. \quad (3.1.75)$$

Here σ_1 may be thought of as the rms extinction error for one extinction observation.

Combining Eqs. (3.1.61) and (3.1.64), we have

$$\sigma^2 = \sigma_{\text{obs}}^2 + \sigma_z^2 + \sigma_M^2 \cdot \sigma_1^2; \quad (3.1.76)$$

σ_{obs}^2 and σ_z^2 may be approximated in terms of the air-mass-dependent error law:

$$\sigma_z^2 \approx \sigma^2(\bar{M}_{\text{ext}})/n_{\text{ext}}, \quad (3.1.77)$$

assuming the extinction stars are used to set the zero point, and

$$\sigma_{\text{obs}}^2 \approx \sigma^2(\bar{M}^*)/n_{\text{prog}}. \quad (3.1.78)$$

Now n_{ext} and n_{prog} , the number of observations of the extinction and program stars, respectively, are in the ratio

$$n_{\text{ext}}/n_{\text{prog}} = F/(1 - F). \quad (3.1.79)$$

Thus, Eq. (3.1.76) becomes

$$\sigma^2 = \frac{\sigma^2(\bar{M}^*)}{N(1 - F)} + \frac{\sigma^2(\bar{M}_{\text{ext}})}{NF} + \frac{\sigma_M^2 \sigma_1^2}{NF}, \quad (3.1.80)$$

where N is the total number of observations. To find the optimum value of F , we set $d\sigma^2/dF = 0$: we find

$$F/(1 - F) = [\sigma^2(\bar{M}_{\text{ext}}) + \sigma_M^2 \sigma_1^2]^{1/2} / \sigma(\bar{M}^*), \quad (3.1.81)$$

or

$$F = \frac{[\sigma^2(\bar{M}_{\text{ext}}) + \sigma_M^2 \sigma_1^2]^{1/2}}{[\sigma^2(\bar{M}_{\text{ext}}) + \sigma_M^2 \sigma_1^2]^{1/2} + \sigma(\bar{M}^*)}. \quad (3.1.82)$$

There are too many independent variables involved in Eq. (3.1.82) to allow any universally applicable conclusions to be drawn (note that the air-mass dependence of the random error law is involved in both σ_1 and \bar{M}_{ext} , and that M_c is involved in \bar{M}^*). However, the two examples used previously may be useful: pure scintillation noise; and scintillation plus a large fixed error, such as occurs in the *UBV* standard stars.

In the first example, Eq. (3.1.12) applies, with $p \approx 2$. We shall assume $f = \frac{2}{3}$, in accord with common practice, and then have $M_2 \approx 2.2$ for best extinction measurement, if $M_1 = 1$. Equation (3.1.12) then gives

$\sigma_1^2 = 26.5 \epsilon_0^2$; we already have $\bar{M}_{\text{ext}} = 1.1$; and $M_c \approx 2.5$ gives $\bar{M}^* \approx 1.3$ for moderate latitudes, and also $\sigma_M \approx 0.4$. Thus $\sigma(\bar{M}_{\text{ext}}) = 1.21 \epsilon_0$, and $\sigma(\bar{M}^*) = 1.69 \epsilon_0$. These values give $F/(1 - F) = 1.41$, or $F = 0.59$. Thus, in this case, each extinction star should receive 1.41 times as much attention as each program star. As each extinction star would normally be observed 3 times per night (rising, setting, and at culmination), each program star should be observed about twice, on the average. To indicate the actual precision involved, the values of ϵ_0 given in Table I of Part 2 can be inserted into Eq. (3.1.12) with $n = 3$: we find $\sigma_A \approx 0.003$ mag/air mass for a 40-cm (16-in.) telescope, and about 0.001 mag/air mass with a 150-cm (60-in.). Thus, the extinction *can* be determined very precisely from just a few observations; the major practical requirement is to provide enough extinction measurements per hour to monitor the temporal changes in the extinction coefficient with adequate accuracy. Finally, we note that a final precision of a few thousandths of a magnitude should be reached.

Now consider the case where large random errors of fixed size occur, as in Hardie's method. We suppose that a fixed random error of 0.02 mag (rms) is present in the standard (extinction) stars, but that only scintillation noise [say, for a 40-cm (16-in.) aperture] affects the program stars. In order to avoid the large *systematic* errors at large zenith distances, we take $M_2 = 4$. The large standard-star error forces us to adopt $f \approx \frac{1}{2}$; so from Eq. (3.1.60) we find $\sigma_A = 0.0104$ mag/air mass, for $n = 2$. Thus $\sigma_1 = 0.0073$ mag/air mass. Because the standard stars are dominated by the large constant error, $\sigma(\bar{M}_{\text{ext}})$ is very nearly 0.02 mag; however, we may take $\sigma(\bar{M}^*) \approx 0.0014$ mag, because program stars are affected only by scintillation noise. If we again adopt $\sigma_M \approx 0.4$, we have $F \approx 0.94$ —in other words, between 14 and 15 standard stars should be observed for one program star! The inefficiency of using the *UBV* "standards" for extinction determination is manifest; in this case, it is impractical to determine the extinction thoroughly and accomplish anything else. (It should be borne in mind that the situation is even worse for larger telescopes.)

Thus, the use of the relatively imprecise *UBV* standard stars for measuring the extinction causes the observer to throw away most of the statistical weight in his raw data. Evidently, much higher precision should be attained by directly measuring the extinction in the natural system of the photometer. Of course, improved precision of the standard stars (i.e., a revised standard system) might help; but it has not yet been

demonstrated that transformations between such broadband systems can be made with the requisite accuracy (a few thousandths of a magnitude) to allow even a revised set of standard values to replace direct instrumental measurements of extinction.

3.1.8. Concluding Remarks on Extinction

If the inherent precision of modern photoelectric observations is to be realized in the final published results, accurate measurements of (and corrections for) atmospheric extinction are necessary. Such measurements can readily be made, with relatively few observations, if proper attention is paid to both instrumental and observational technique, and if the reduction methods are properly matched to the observations. In particular, one should have:

- (1) temperature regulation of *all* spectrally selective components (filters, receiver, and standard source) to a few tenths of a degree;
- (2) a large enough focal-plane diaphragm to include essentially *all* the light of a star, at *all* zenith distances, to avoid seeing-dependent effects;
- (3) no observations at altitudes below about 20° ;
- (4) frequent-enough observations of extinction stars to monitor changes in extinction with adequate accuracy; and
- (5) a realistic reduction and weighting scheme, preferably based on actual, measured characteristics of the instrument used.

If the extinction is determined from *UBV* "standard" values, it is difficult to achieve adequate precision. However, if the extinction is measured directly in the instrumental system, only enough observations are needed to measure the time dependence of the extinction. For example, if 15 stars/hr can be observed, about 5 of these should be extinction stars. If each extinction star is observed 3 times (once each rising, setting, and at transit), adequate coverage is achieved by selecting one extinction star for each 35 min of right ascension from the declination zone that passes within 20° of the observer's zenith. If the observer knows from past experience that changes in extinction are unlikely to occur, and/or is willing to discard nights on which significant changes exist, the number of extinction stars might be reduced to 1/hr of R.A. (three observations per hour of time). It does not appear wise to reduce the density of extinction stars below this level, which is already quite low (only 20% of all observations).

Finally, the accuracy of the results depends on an accurate modeling of instrumental and atmospheric characteristics in the reductions. This means the use of an accurate air-mass formula (bearing in mind that *no* formula is accurate beyond two or three air masses); a physically based (rather than empirical) correction for bandwidth (color-dependent) effects; a proper choice between "colors" and "magnitudes" as observational variables; reduction of several nights together, if instrumental stability permits; and a realistic weighting scheme.

It appears that if the work is carefully done, ground-based photometry with a real accuracy of a few thousandths of a magnitude should be possible.

3.2. Transformation to a Standard System

3.2.1. Introduction

The previous sections show how to obtain reproducible photometric data and reduce them to outside the earth's atmosphere. These reduced data, however, are still on the natural system of the photometer, that is, they are measurements made with the spectral response function of a *particular* instrument. In most cases, one needs to compare and combine observations made with *different* instruments. Thus we must "transform" the instrumental magnitudes and colors to the values that would have been measured with a *standard* instrument, having a different spectral response.

Usually in astronomy, this is a real instrument which has measured magnitudes and colors for a rather small list of "standard" stars. This is a practical procedure because (a) many stars are in fact quite constant over long periods of time, and (b) by using these measured objects as standard lamps, there is no need to know the actual spectral response of the instrument to perform the transformation. The latter is a very important point; for (as explained in Section 2.2.1.1) absolute comparisons with laboratory standards are much more difficult and less precise than comparisons between stars.

On the other hand, laboratory photometry is based on the tabulated spectral response function of a mythical "standard observer," so that, in principle, one must know the instrumental spectral response (and match it²³ to that of the standard observer). This does not lead to a precisely reproducible system, both because of the difficulties in making the

²³ H. Wright, C. L. Sanders and D. Gignac, *Appl. Opt.* 8, 2449 (1969).

necessary absolute measurements of spectral response, and because the standard response function is not well defined between tabulated wavelengths (different interpolation schemes give different intermediate values).

At first, these two approaches seem quite different, but they turn out to have many features in common. First, it is still highly desirable to know the spectral response functions of standard astronomical systems, so that model-atmosphere fluxes can be compared directly with observed colors. This is closely related to the problems of establishing the stellar effective-temperature scale, and of determining bolometric corrections. Second, it turns out that matching the instrumental response to that of the standard system is as important astronomically as in laboratory photometry, because of difficulties in transformation. And finally, both the laboratory photometric units and "visual" stellar magnitudes^{24,25} are historically based on measurements made with the human eye; the major difference is that the laboratory units are based on the eye's bright-adapted (photopic) spectral response, but the astronomical systems are based on the mesopic or scotopic (dark-adapted) response, which is shifted to shorter wavelengths. Thus the effective wavelength of laboratory photometry is near 5550 Å, while that of the *V* magnitude^{24,25} is near 5400 Å.

3.2.2. Transformations for Blackbodies

3.2.2.1. Temperature Reddening. If we assume that the major difference between instrumental and standard systems is one of effective wavelength, the transformation can be done accurately for blackbodies. Because many stellar and laboratory sources have nearly blackbody spectra, this is a useful and instructive result.

The Planck formula for the blackbody flux per unit frequency interval is

$$F_\nu = 2\pi h\nu^3 c^{-2} / [\exp(h\nu/kT) - 1], \quad (3.2.1)$$

so the monochromatic magnitude of a blackbody is

$$\begin{aligned} m_\nu &= -2.5 \log_{10} F_\nu(T) + \text{const} \\ &= -7.5 \log \nu + 2.5 \log[\exp(h\nu/kT) - 1] + \text{const}. \end{aligned} \quad (3.2.2)$$

^{23a} H. F. Weaver, *Popular Astron.* 54, 211, 287, 339, 389, 451, 504 (1946).

²⁴ R. V. Willstrop, *Mon. Notices Roy. Astron. Soc.* 121, 17 (1960).

²⁵ A. Ažusienis and V. Straizys, *Bull. Vilnius Astron. Obs.* No. 16, p. 3; No. 17, p. 3 (1966). See also *Sov. Astron.-AJ* 13, 316 (1969).

At the high-frequency side of the curve $\exp(h\nu/kT) \gg 1$, so we can adopt the Wien approximation [drop the 1 in Eq. (3.2.2)] and write

$$m_\nu \approx -7.5 \log \nu + 1.08h\nu/kT + \text{const.} \quad (3.2.3)$$

Over a modest frequency interval, the curvature of $\log \nu$ is small, so m_ν is nearly a linear function of ν ($= c/\lambda$). Thus if we have observed monochromatic magnitudes m_1 and m_2 of a blackbody at frequencies ν_1 and ν_2 , the magnitude m_* at some nearby frequency ν_* can be found by linear interpolation or extrapolation:

$$\begin{aligned} m_* &= m_1 + \left(\frac{\nu_* - \nu_1}{\nu_2 - \nu_1} \right) (m_2 - m_1) \\ &= m_1 + \alpha(m_2 - m_1). \end{aligned} \quad (3.2.4a)$$

If we know the frequencies ν_1 , ν_2 , and ν_* , we can calculate the transformation coefficient α ; however, if we do not, it can be found empirically from measurements of the same blackbody at all three frequencies.

We note that $(m_2 - m_1)$ in Eq. (3.2.4a) is a color index; thus the last term is usually called the *color term* in the transformation. If the magnitude scales are defined with arbitrary (e.g., instrument-dependent) zero-point constants [on the right sides of Eqs. (3.2.2) and (3.2.3)], we will also have a *zero-point term* in Eq. (3.2.4a) which becomes

$$m_* = m_1 + \alpha(m_2 - m_1) + \beta. \quad (3.2.4b)$$

There are now *two* transformation coefficients (α and β) to be determined. If this is done empirically, we must observe at least two blackbodies of different colors (i.e., temperatures) to find α and β .

Finally, if we measure in two narrow frequency bands ν_{1*} and ν_{2*} , we can write down two transformations similar to Eq. (3.2.4b), and by subtraction find the linear transformation between the starred and the unstarred color indices:

$$(m_{2*} - m_{1*}) = \gamma(m_2 - m_1) + \delta. \quad (3.2.5)$$

Again, the transformation involves only a linear color term and a zero-point term, which may be either computed from the definitions of the four magnitude systems, or found empirically. The coefficient γ , like α , is just the ratio of frequency differences (or "color baselines") for the starred and unstarred systems; in fact, Eq. (3.2.4b) is a special case of Eq. (3.2.5) with $m_{1*} = m_1$, and $m_{2*} = m_*$.

3.2.2.2. Atmospheric and Interstellar Reddening. In the approximations above, the monochromatic magnitudes of blackbodies are linear functions of $1/\lambda$. Any selective extinction or *reddening* that is also (in stellar magnitudes) a linear function of $1/\lambda$ will be indistinguishable from a change in blackbody temperature. In particular, the interstellar reddening is nearly proportional to $1/\lambda$ in the visible spectrum. Thus linear color transformations are as applicable to reddened stars as to unreddened ones.

Furthermore, the aerosol component of atmospheric extinction is also approximately proportional to $1/\lambda$; and, over a limited wavelength interval, the Rayleigh extinction in magnitudes (proportional to $1/\lambda^4$) can be approximated by a linear function of $1/\lambda$. [For example, a Taylor series expansion about λ_0^{-1} gives

$$\lambda^{-4} \approx \lambda_0^{-4} + 4\lambda_0^{-5} \left(\frac{1}{\lambda} - \frac{1}{\lambda_0} \right) = (4\lambda_0^{-5}) \left(\frac{1}{\lambda} \right) - 3\lambda_0^{-4}.]$$

Thus we expect the monochromatic extinction correction—regarded as a transformation between intra- and extra-atmospheric systems, at a fixed air mass—to be approximately a linear function of $1/\lambda$. In this approximation, atmospheric reddening (like interstellar reddening) is indistinguishable from temperature reddening; only our ability to calculate the air mass and its effect allows us to correct for the atmosphere.

If all reddening is equivalent to temperature reddening, each object can be assigned a unique color temperature T_c . Then Eq. (3.2.2)–(3.2.5) show how measurements at different spectral frequencies are related. Since only one parameter (a color, or a color temperature) is involved, the *same* transformation applies to all objects, reddened and unreddened. To the extent that *broad-band* magnitudes can be regarded as shifted in effective wavelength by the addition of a colored filter (a fixed mass of reddening atmosphere), their transformation to outside the atmosphere should contain a linear color term; Eq. (3.1.57) shows that it does (namely, the term in ΔX).

How valid are these linear one-color transformations? To derive them, we have assumed (a) blackbody sources; (b) the Wien approximation; (c) monochromatic measurements; and (d) $|\nu_1 - \nu_2| = \Delta\nu \ll \nu$, so that curvature in $\log \nu$ can be neglected. However, if $\Delta\nu \ll \nu$, we can assume m_ν is a linear function of ν without the Wien approximation. Furthermore, if our sources have sufficiently smooth spectra, we can assume linearity of m_ν even if the sources are not blackbodies. Thus linear transformations should be valid for any such sources, provided that $\Delta\nu \ll \nu$.

However, the spectra of real astronomical sources are not perfectly smooth, but have absorption and/or emission features. Furthermore, most astronomical color systems have $(\Delta v/v) \approx 0.1$ or 0.2 , i.e., not very small. Consequently, such transformations are not sufficiently accurate to preserve the inherent precision (<0.01 mag) of good photoelectric photometry.

We can improve the transformation empirically by using additional data. For example, if we have measurements in 3 bands instead of 2, we can use a formula like

$$m_* = m_1 + \alpha(m_2 - m_1) + \beta(m_3 - m_2) + \gamma. \quad (3.2.6)$$

This has worked fairly well in some cases, e.g., where m_* is the red-leak of the U filter, and the numbered bands are U , B , and V ; however, it fails for cool^{25a} or reddened²⁵ stars. As a second example, both Schmidt-Kaler²⁶ and Fernie and Marlborough²⁷ have found systematic transformation errors that are proportional to interstellar reddening. For O and B stars, the reddening is a linear combination of $(U - B)$ and $(B - V)$, so Eq. (3.2.6) applies; but for later spectral types, a different, nonlinear relation is required. As a final example, Argue²⁸ used equations like (3.2.6) to transform his observations of late-type stars, but found that systematic differences between luminosity classes remained.

Clearly no linear, single-valued transformation is accurate enough to preserve the full weight of good data. Every phenomenon we wish to measure—temperature, luminosity, reddening, and probably also metallicity, rotation, and other peculiarities—seems to require a different photometric transformation. Of course, a careful spectral analysis of each star would provide this information, but this is self-defeating: one of the main goals of multicolor photometry is to provide such data *without* requiring spectra.

3.2.3. Transformations in General

3.2.3.1. The Problem. Must we then abandon hope of preserving observational accuracy through the transformation to a standard system? To answer this, we must look more closely at the general transformation problem. We saw that blackbody data could be transformed accurately

^{25a} C.-Y. Shao and A. T. Young, *Astron. J.* **70**, 726 (1965).

²⁶ T. Schmidt-Kaler, *Observatory* **81**, 246 (1961).

²⁷ J. D. Fernie and J. M. Marlborough, *Observatory* **84**, 33 (1964).

²⁸ A. N. Argue, *Mon. Notices Roy. Astron. Soc.* **125**, 557 (1963).

because they form a one-parameter family of spectral distributions. If interstellar reddening, for example, were identical to temperature reddening, they would be indistinguishable, and the same transformation would apply to both reddened and unreddened stars. In fact, they are not: the spectral features (Balmer decrement and interstellar slope change near 4500 Å) that permit us to separate interstellar reddening from temperature effects in early-type stars are the very features that produce different transformation relations for the two groups. Each additional effect, such as metallicity, luminosity, or rotation, must leave its signature in the stellar spectrum, and hence in the transformation from one response curve to another. The *ad hoc* treatment of each effect separately is not very satisfactory, not only because it requires a huge number of standard stars of different luminosity, reddening, etc., but also because it leaves unsolved the problem of transforming peculiar objects (pulsars, quasars, galaxies, planets, emission-line stars, nebulae, . . .) to a common basis. Furthermore, these *ad hoc* treatments are in principle unable to cope with the general problem of transforming observations of arbitrary spectral distributions, because the set of all possible spectra (one-valued functions) is larger than a countable infinity, so that even a (countably) infinite number of individual treatments is inadequate.

Another way²⁹ of viewing the transformation problem is to regard a spectrum as a point or vector in an infinite-dimensional space: the coordinates of the point, or components of the vector, are the spectral power densities at successive wavelengths. A photometric measurement in m different bands projects or maps the infinite-dimensional vector into an m -dimensional subspace. Two such mappings can be mapped into each other in a one-to-one way (i.e., two photometric systems are related by a single-valued transformation) if the subspaces are linearly dependent; the transformation then amounts to a rotation of axes in m -dimensions. However, if one of the subspaces contains an appreciable component orthogonal to the other subspace, this represents spectral information not contained in the other, which is excluded by any transformation between them. Thus two photometric systems are transformable if and only if the response functions of one are a linear combination of the response functions of the other.

The concepts of linear dependence and information content suggest an information-theory approach, as follows. Suppose we treat the general problem of photometric transformations in a manner analogous to

²⁹ G. H. Conant, Jr., Private communication (1959).

King's treatment¹⁶ of the extinction correction (i.e., the transformation of broad-band data from inside to outside the atmosphere). King showed that transformations between different systems depend on derivatives of the energy distribution $S(\lambda)$ reaching the photometer, and on the second (and higher) moments of the instrumental response function $\phi(\lambda)$ about some effective wavelength λ_1 . The leading terms in the Taylor series expansion about λ_1 depend on $[d(\ln S)/d(\ln \lambda)]$ and the mean square bandwidth w^2 . In practice, we must approximate this unknown derivative by a color index [cf., Eq. (3.1.51)].

However, different reddening mechanisms generally produce different relations between $[d(\ln S)/d(\ln \lambda)]$ and a color index which depends on a second band centered at λ_2 . We can write the color index in stellar magnitudes as

$$C_{12} = 1.086[\ln S(\lambda_2) - \ln S(\lambda_1)] \quad (3.2.7)$$

and, expanding $(\ln S)$ in a Taylor series at λ_1 , we have

$$\begin{aligned} \ln S(\lambda_2) - \ln S(\lambda_1) &= \frac{d(\ln S)}{d(\ln \lambda_1)} \cdot (\ln \lambda_2 - \ln \lambda_1) \\ &+ \frac{d^2(\ln S)}{d(\ln \lambda_1)^2} \cdot (\ln \lambda_2 - \ln \lambda_1)^2 + \dots \end{aligned} \quad (3.2.8)$$

The first term in Eq. (3.2.8) is the theoretical justification for replacing the logarithmic derivative by a color index. However, in fact, the second (and higher-order) terms are appreciable in accurate photometry, and differ for different reddening mechanisms. These terms would be small if $S(\lambda)$ were a sufficiently "smooth" function. However, these terms are quite large if $S(\lambda)$ has a kink near λ_1 —such as the Balmer jump in U , or the interstellar reddening break in B . These higher-order terms spoil the uniqueness of the transformation in terms of a color index, and explain why different relations are required for stars of different reddening and luminosity.

Making the bands narrower does not solve the problem, because then individual spectral features play a larger part in proportion to the band width, and small instrumental wavelength shifts due to temperature variations and manufacturing tolerances become more important. Placing the bands closer together helps, because of the powers of $[\ln(\lambda_2/\lambda_1)]$ which appears in the higher terms of Eq. (3.2.8). However, discrete bands cannot be placed close enough together to solve the problem, even if they are adjacent; for we can always encounter spectral distributions which give the same *response* in each band, but have very different

gradients *across* each band. Thus, cutting the spectrum up into adjacent rectangular passbands, no matter how small, does not provide enough information to solve the transformation problem.

At first glance, it may appear that since adjacent rectangular passbands measure all the power in a spectrum, no more information can be obtained, and the problem is insoluble. This is not the case, and we shall show that a completely satisfactory solution is readily attainable. To do this, we adopt a more fundamental point of view: we regard multicolor photometry as low-resolution spectroscopy.

3.2.3.2. The Solution: A Spectroscopic Approach. Suppose we want to determine the energy distribution in a star's spectrum at some low resolution—say, 500 Å, which would yield a function $S^*(\lambda')$. Here λ' is the varying center wavelength of the spectral window, and the asterisk indicates the effect of smearing the spectrum out by the slit function $W(\lambda - \lambda')$.

We could equally well measure the spectrum by using a Michelson interferometer.³⁰ The resulting interferogram (output intensity as a function of path difference) is the Fourier transform of the spectrum; if we only need low resolution, we need only measure the central part of the interferogram (small path differences). In fact, the interferogram (Fourier transform) of S^* is just the product of the Fourier transforms of S and W .

We must realize that, as we actually only measure a part of the spectrum, and a part of the interferogram, the measured finite parts are not exact Fourier transforms of each other. However, we can choose W so that a reasonably short piece of the interferogram transforms into S^* as accurately as we wish. In particular, we can determine the values of S^* and its derivatives at every point in the spectrum, well enough to transform our measurements to any photometric system which does not exceed the spectral resolution of our data.

In fact we can do this without using either a spectrum scanner or an interferometer, by making regular photometric measurements through a series of filters having $W(\lambda)$ as the passband shape. To prove this assertion, we regard $S^*(\lambda)$ as a real function on some interval (λ_1, λ_2) . Let its interferogram (Fourier transform) be

$$s^*(\omega) = (2\pi)^{-1/2} \int_{\lambda_1}^{\lambda_2} S^*(\lambda) \exp(i\omega\lambda) d\lambda, \quad (3.2.9)$$

³⁰ L. Mertz, "Transformations in Optics." Wiley, New York, 1965.

where the interferogram "frequency" ω is not to be confused with optical frequency c/λ . Now if we have chosen $W(\lambda)$ so that its transform $w(\omega)$ is negligible for $|\omega| > \omega_{\max}$, we guarantee that $s^*(\omega)$ is also negligible outside this range, even if $S(\lambda)$ consists of delta functions (emission lines!). Then the sampling theorem³¹ tells us that S^* is completely specified by its values at λ_1 , $\lambda_1 + \pi/\omega_{\max}$, $\lambda_1 + 2\pi/\omega_{\max}$, These sampled values are simply photometric observations with filters spaced $\Delta\lambda = \pi/\omega_{\max}$ apart in wavelength, as stated above.

In other words, we can render even an emission-line spectrum transformable to a standard system if we smear it out adequately by choosing a suitable passband shape. Also, if we can handle emission nebulae, we can certainly handle any star, no matter how peculiar. A special advantage of such a system is that the *same* transformation applies to all objects, regardless of spectral peculiarities. Thus a small number of ordinary stars can be used as standards.

The requirement that $s^*(\omega)$ be negligible beyond ω_{\max} is necessary to achieve accuracy in the reconstruction of S^* from the samples. Any harmonics beyond ω_{\max} will appear in the sampling as though they were at image frequencies less than ω_{\max} such as $|2\omega_{\max} - \omega|$, $|4\omega_{\max} - \omega|$, etc., a phenomenon known as *aliasing*. That is why we must choose $W(\lambda)$, and hence $w(\omega)$, so as to prevent these images from appearing in $s^*(\omega)$. We cannot make them vanish, but we can make them very small beyond some point; this is a standard problem in one-dimensional apodization.³² For the *UBV* bands, frequencies ω far beyond the sampled limit $\omega = \pi/\Delta\lambda$ are still important, and we may regard the *UBV* difficulties as due to the aliasing of these frequencies into the sampled frequency range.

To ensure that all transformation errors are less than some fraction f , it suffices to require that the sum of the amplitudes of all Fourier components with $\omega > \omega_{\max}$ be less than f , that is,

$$\int_{\omega_{\max}}^{\infty} |w(\omega)| d\omega / \int_0^{\infty} |w(\omega)| d\omega \leq f. \quad (3.2.10)$$

This condition cannot be met for a rectangular passband, whose amplitudes fall off only as ω^{-1} . [We should have seen this from the Gibbs

³¹ R. W. Ditchburn, "Light," 2nd ed., chapter 20. Wiley (Interscience), New York, 1963.

³² P. Jacquinot and B. Roizen-Dossier, in *Progr. Opt.* **3**, 31-184. See also A. Papoulis, *J. Opt. Soc. Amer.* **62**, 1423 (1972).

phenomenon, which results from truncating $w(\omega)$ if $W(\lambda)$ is discontinuous. Another example is the ringed diffraction pattern of a telescope with sharp-edged pupil.] Rectangular-passband photometry is clearly nontransformable, for if a spectral line falls into one band and is excluded from the next, there is no way to interpolate the result for an intermediate band: the line is either in or out, but we cannot say which.

However, Eq. (3.2.10) can be satisfied by continuous band profiles; the smoother the profile, the more rapidly $w(\omega)$ becomes negligible, and the farther apart in wavelength the bands may be placed. For example, the sinusoidally modulated or "channelled" spectrum used by Walraven³³ allows bands to be spaced approximately $\Delta\lambda = 1.11f^{1/2}\lambda_w$ apart, where f is the maximum transformation error and λ_w is the full width between minima of the spectral channel. Thus for $f = 0.01$, $\Delta\lambda \approx \lambda_w/9$, which is just under $\frac{1}{4}$ of the full width of a channel at half response.

This may seem a close spacing; but the problem is considerably worse with most glass or interference filters, which give steep-sided or asymmetric passbands with higher harmonic content (bigger Fourier components at large ω). The deeply overlapping bands required for accurate transformation may look redundant at first glance, but the sampling theorem shows that they are not—in fact, they provide just enough pieces of independent information to allow accurate transformations. One can show, for example, that steep-sided filters like those of the *UBV* system must be spaced about 100 Å apart to allow accurate transformation. Hence the observed transformation errors represent severe aliasing, due to undersampling by about a factor of 10. The same problems must also occur with the numerous narrower-band systems that have been introduced, as they also have poor overlap between bands.[†]

3.2.4. Matching Response Functions

Until inherently transformable systems are in general use, the photometrist's best hope is to measure his response functions, and, by choosing appropriate filters and detectors, match them as closely as possible to the standard response functions (if these are known). The results of trial-and-error matching are reported by Hardie;⁴ methods of designing

³³ T. Walraven, *Bull. Astron. Inst. Netherlands* **15**, 67 (1960).

[†] Systematic transformation errors "up to several hundredths of a magnitude" have been found in the Strömberg *wavy* system [J. A. Graham and Arne Slettebak, *Astron. J.* **78**, 295 (1973).]

a close match are given by Wright *et al.*²³ The *UBV* response functions are not accurately retrievable; a most careful reconstruction has been done by the Vilnius group.²⁶ The authors of newer systems have been somewhat more careful in measuring filter passbands, but other instrumental factors (transmission, and detector response) are often neglected. The narrow-band systems may be more difficult to reproduce, because of steep-sided and ripple-topped interference filters; also, a 10-Å error is a larger fraction of the bandwidth of a 100-Å filter.

To duplicate existing systems with the greatest accuracy, it should prove helpful to use two instrumental bands similar in shape to the standard, but differing in effective wavelength by a small fraction of the band width, such as a pair of Hardie's "visual" filters. Interpolation between these, using the short-baseline color they define, should give a much more accurate transformation to a standard system than does the usual transformation using long-baseline (i.e., equal to or exceeding the band width) colors. Of course, this doubles the labor of measurement. However, halving the duration of each observation would leave the total time fixed. The resulting $2^{1/2}$ increase in random errors may be a small price to pay for a large decrease in systematic transformation errors, if (as is often the case) the latter are the more important.

3.2.5. Mathematical Models

In King's analysis of the extinction transformation,¹⁰ the measured quantity is expanded in a series whose terms are products of (a) the central *moments* [such as w^n in Eq. (3.1.45)] of the instrumental response function, and (b) the wavelength *derivatives* (such as N and n) of the stellar spectrum and of the atmospheric extinction. High-order terms in this series can be neglected if, with increasing order, the instrumental moments decrease (which means using sufficiently narrow bands) and the atmospheric derivatives remain moderate (which means avoiding regions of molecular absorption).

The major problem with existing systems is that color indices formed from undersampled spectral data provide a poor estimate of the spectral gradient N within each band. If adequately sampled data were used, the linear approximations derived above should be quite accurate, both for the color term in the extinction and for the color terms in transformation from instrumental to standard systems. In the case of the instrumental factors, we note that two types of deviations from the standard response functions occur. The first, contributed primarily by the ratio of response

curves of the standard and instrumental photomultipliers, is a smooth function,³⁰ like the atmospheric transmission. We already know from King's analysis that a linear color term takes care of this very well. The second problem is the displacement of filter cutoffs from their standard wavelengths, due to manufacturing errors or temperature shifts. This alters the effective wavelength of an instrumental passband; but a linear color transformation is adequate to correct for this if Eq. (3.2.10) is satisfied. However, even if adequate sampling is used, a formula involving several color indices, such as Eq. (3.2.6) may be required; if n adjacent bands overlap, it seems best to use an n -point interpolation formula to reduce them to the standard magnitude m_* at frequency ν_* . Undersampled data will generally require nonlinear terms to allow, in part, for aliasing.

Whatever analytical form is chosen to represent the data, there remains the statistical problem of finding the best coefficients to use in this formula. A blind application of least squares may produce systematic errors, as the following example shows: Suppose we make two different sets of measurements of the same stars with the same photometer, which remains absolutely unchanged between the two series. Owing to experimental errors, the values obtained for the same star will be slightly different in the two series; how do we combine them? Now, we know the two sets are on the same photometric system, so that in Eq. (3.2.5), for example, we must have $\gamma \equiv 1$ and $\delta \equiv 0$. However, we also know from linear regression theory that the expected least squares value of γ will be less than unity (and $\delta > 0$) because of the imperfect correlation produced by the random errors. Thus a least squares fit of one set of data to the other will produce systematic errors, which depend on the relative sizes of the errors in the two sets of data.[†] Other systematic effects arise because of partially correlated errors between terms with a common element [e.g., V and $(B - V)$, or $(B - V)$ and $(U - B)$.] Such problems (and their solutions) are discussed at length by Deeming,³⁴ who shows that systematic errors of 0.005 mag in $(B - V)$ are readily attained in ordinary photometry.

Such systematic errors are serious enough in themselves, for they are larger than the random errors of good observations. However, they can become multiplied severalfold in some situations. For example,

³⁴ T. J. Deeming, *Vistas Astron.* 10, p. 125.

[†] Such a situation exists between "summer" and "winter" *UBV* standard stars.²⁵

photometry of a faint variable star in a globular cluster or nearby galaxy may be done photographically, relative to comparison stars which have also been calibrated photographically, against faint (~ 17 mag) photoelectric standards, which in turn are related to brighter "secondary standards" (~ 10 mag), which have been transformed to match some bright "standard stars" that were originally tied to a few "primary standards." Often a big telescope is used for the faint stars, but the brighter "secondary standards" have been set up using a smaller telescope. Thus the faint stars on which the distance scale hangs are separated from bright nearby standards by 3 or 4 transformations, with cumulative systematic errors at each step. As the systematic effects depend on the squares of the random errors, they can be quite large at the faint end of the scale. These transformation errors, of course, are in addition to any scale errors due to nonlinearity over a large dynamic range.

Thus, as in correcting for extinction, the photometrist must carefully match his mathematical techniques to the actual situation at hand. A poor choice of model, or misuse of least squares, can produce large systematic errors, even with small residuals.

4. RESHAPING AND STABILIZATION OF ASTRONOMICAL IMAGES*

4.1. Reshaping of Images

4.1.1. Definitions

The terms used to describe pencils of radiation differ between astronomers and optical physicists. Table I shows the equivalences, and illustrates the potential confusion due to different uses of the same word. The astronomical terms will be adopted here. The task of the astronomical spectroscopist is to gather the maximum possible radiant power from a

TABLE I. Comparison of Terminologies Used in Astronomy and Optics^a

Astronomy	Optics	Units
1. (Specific) intensity	Radiance, brightness	$\text{erg cm}^{-2} \text{sr}^{-1} \text{sec}^{-1}$
2. Flux	(Illumination, emittance)	$\text{erg cm}^{-2} \text{sec}^{-1}$
3. (Radiant power)	Flux	erg sec^{-1}
4. (Luminosity/ 4π)	Intensity	$\text{erg sr}^{-1} \text{sec}^{-1}$

^a Parentheses indicate that the correspondence is not exact, or that the term is not standard.

given source, and to disperse and detect it appropriately. A useful parameter of a telescope or spectroscope is its *throughput*, the product of area A and solid angle Ω that the instrument accepts. (Other terms in use are *étendue*, *light-gathering power*, and *luminosity*; the last seems especially inappropriate because of its other meanings.) The solid angle for a sizable telescope can usefully be taken as that of a typical seeing disk under moderately good conditions, that is, a circle of 1-arcsec radius, or 7.4×10^{-11} sr. Refined work on extended sources, such as the sun and

* Part 4 is by Donald M. Hunten.